Agents affecting the apoptotic process by influencing the mitochondrial permeability transition

Gabor Varbiro, M.D.

Institute of Biochemistry and Medical Chemistry

Faculty of Medicine

University of Pecs

Ph.D. Program leader: Prof. Balazs Sumegi, DSc.

Contents.

Abbreviations.

DR .... Death Receptor

BH .... Bcl-2 Homology

DD .... Death Domain

MPT .... Mitochondrial Permeability Transition

ROS .... Reactive Oxygen Species

AIF .... Apoptosis Inducing Factor

PTPC .... Permeability Transition Pore Complex

VDAC .... Voltage Dependent Anion Channel

ANT .... Adenine Nucleotide Translocase

Smac .... Second Mitochondrial Activator of Caspases

DIABLO .... Direct IAP-Binding Protein of Low isoelectric point [pI]

IAP .... Inhibitor of Apoptosis

IM .... Inner Membrane

OM .... Outer Membrane

$\Delta\Psi$ .... Mitochondrial Membrane Potential

CsA .... cyclosporine A

Rh123 .... Rhodamine 123

DRh123 .... Dihydrorhodamine 123

Resorufin N-acetyl-8-dodecyl-3,7-dihyroxyphenoxazine

HEPES .... N-2-hydroxyethyl piperazine-N'-2-ethansulfonic acid

MTT^+ .... (3-[4,5-dimethylthiazol-2-yl]-2,5-diphenyl-tetrazolium bromide

PI .... Propidium Iodide

Introduction.

General features of programmed cell death.

Apoptosis, or programmed cell death is recognized as a critical element in the removal of cells following exposure to toxic compounds as well as during development and in degenerative disorders. In general programmed cell death represents a continuum of cell death ranging from classical apoptosis to necrosis at its two poles. Apoptosis is a common and evolutionary conserved mechanism present in most living organism. Tissue homeostasis relies on the tightly controlled removal of superfluous, damaged and ectopic cells through apoptosis. Whereas an aberrant resistance to apoptosis participates in the development of neoplasia, excessive cell death, through apoptosis contributes to acute organ failure as well as to chronic diseases involving the loss of post-mitotic cells.

Recently, much progress has been made towards elucidating the various signal transduction pathways that can ultimately lead to a cell's demise. Based on this information, many apoptotic cascades have been described, such as intrinsic and extrinsic, mitochondrial and death receptor (DR), p53-dependent and independent pathways in association with initiation, commitment and execution phase. It has become increasingly apparent that apoptosis is not a series of series of clearly defined pathways, but rather, a multitude of highly regulated , interconnected pathways. While trying to view any of these pathways in isolation is clearly an oversimplification, the sheer magnitude of possible events makes it a necessity.

The *intrinsic cell death pathway* involves the initiation of apoptosis as a result of a disturbance of intracellular homeostasis. In this pathway, mitochondria are critical for the execution of cell death, and so this pathway has been referred to as the mitochondrial cell death pathway. The *extrinsic pathway* involves the initiation of apoptosis through ligation of plasma membrane DRs, and so this pathway is also referred to as the DR pathway. While the

initiation mechanism of these pathways are different, both converge to result ultimately in cellular morphological and biochemical alterations characteristic of apoptosis. It is also apparent that a considerable interaction between the pathways occur upstream of the convergence point, and that individual cells possess a considerable degree of redundancy in their apoptotic pathways. The main apoptotic cascade components and their most important features are described in the following.

Caspases.

Caspases (cystein apartate-specific proteases) are a family of intracellular proteins involved in the initiation and execution of apoptosis (Wolf and Green, 1999). Their activation is often referred to as the apoptotic commitment point. Caspases are synthesized as procaspases that are then proteolytically processed, at critical aspartate residues, to their active forms. All procaspases contain a highly homologues protease domain as well as an NH_2 terminal prodomain. The induction of apoptosis through extrinsic or intrinsic death mechanisms results in the activation of initiator caspases. DRs, through adaptor molecules, recruit initiator caspases 2, 8, or 10, while intrinsic death signal results in the activation of caspase 9. Activation of initiator caspases is the first step of a highly regulated, irreversible self amplifying proteolytic pathway. Initiator caspases are able to cleave procaspases, and thus are able to activate effector caspases (caspases 3, 6, and 7) or are able to amplify the caspase cascade by increased activation of initiator caspases. Effector caspases are common to both the extrinsic and intrinsic death pathways, and therefore, the ultimate morphological and biochemical hallmarks of apoptosis are relatively independent of the apoptotic inducer.

Bcl-2 family.

Members of the Bcl-2 family of intracellular proteins are essential mediators of cell survival and apoptosis (Cory and Adams, 2002). Both anti- and pro-apoptotic family members have been characterized and their classification is related to the presence or absence of Bcl-2

homology (BH) domains. Four BH domain have been described. Bcl-2 and Bcl-X$_L$ both contain all four BH domain, possess established roles in the inhibition of apoptosis, although their exact mechanism remains elusive. It has been proposed that anti-apoptotic Bcl-2 family members inhibit apoptosis by antagonizing the actions of proapoptotic family members. This antagonism is proposed to occur upstream of apoptosis-related mitochondrial alterations. Two subfamilies of pro-apoptotic Bcl-2 family members have been identified; the bax family (Bax, Bok, and Bak), containing BH1, BH2, and BH3, and the BH3-only family (Bid, Bim, Bik, Bad, Bmf, Hrk, Noxa, and PUMA). Similar to the anti-apoptotic family members, the exact mechanism of action of pro-apoptotic Bcl-2 family members is uncertain.

Death Receptors.

Cell surface DRs belong to the tumor necrosis factor receptor (TNFR) superfamily (Chen and Goddel, 2002). They transmit their apoptotic signals following binding of death ligands. These receptor –ligand complexes initiate apoptotic cascades within seconds of ligand binding and can result in apoptotic cell death within hours. The best characterized family members include Fas (also known as Apo1 or CD95); additional members are DR3 (or Apo3), DR4, DR5 (or Apo2), and DR6. These receptors are Type I transmembrane receptors characterized by extracellular cysteine-rich domains (CRD) and intracellular death domains (DDs). The DD consists of six antiparallel, amphipathic α-helices folded in a configuration that results in the surface exposure of a number of charged residues. Following receptor-ligand binding, receptor DDs interact. Subsequent to this activation of DRs, other DD-containing proteins are recruited and function as adaptor proteins in the signal transduction cascade. These adaptor proteins interact with a variety of other proteins to complete the DR signaling pathways.

The role of mitochondria in apoptosis.

The *intrinsic cell death pathways* follow from proapoptotic signals resulting in a disruption of intracellular homeostasis, that is the signals for cell suicide originate within the cell (Green and Reed, 1998; Wang, 2001). The mitochondria are the primary intracellular initiation sites although the endoplasmatic reticulum has also been implicated. All cells harbor the latent ability to undergo programmed cell death. Under normal circumstances, apoptosis is suppressed, as a result of the rigorous compartmentalization of catabolic enzymes and their activators. Mitochondria play a major role in this subcellular partitioning of death-regulating biochemical signals (Penninger and Kroemer, 2003). For example, cytochrome *c* is confined to the mitochondrial intermembrane space preventing it from interacting with apoptotic-protease-activating factor 1 (Apaf-1), a cytosolic protein. Upon permeabilization or rupture of the outer mitochondrial membrane, cytochrome *c* binds to Apaf-1, leading to allosteric activation of procaspase-9. Caspase-9 then proteolytically activates caspase-3, one of the principal proteases that participates in the execution of cell death. Similarly, Smac/DIABLO (second mitochondrial activator of caspases/direct IAP-binding protein of low isoelectric point [pI]) and Omi/HtrA2, two intermembrane proteins, are normally physically separated from cytosolic inhibitors of apoptosis proteins (IAPs). Upon mitochondrial permeability transition (MPT), Smac/DIABLO and Omi/HtrA2 neutralize IAPs, and thus relive the IAP-mediated inhibition caspase-3 and −9. Two DNA-destroying enzymes, apoptosis inducing factor (AIF) and endonuclease G, are also normally confined to the mitochondrial intermembrane space, but following MPT they can move to the nucleus where they mediate chromatinolysis.

Mitochondrial Permeability Transition (MPT).

MPT is a major event in physiological as well as pathological cell death, and not surprisingly, it is regulated at multiple levels (Zamzami et al., 1996). MPT can be induced by multiple pro-apoptotic second messengers (Fig. 1.), including Ca^{2+}, reactive oxygen species (ROS), lipid messengers (e.g. ceramide and ganglioside GD3) and stress kinases. In addition it is facilitated by pro-apoptotic proteins from the Bcl-2 family, and is inhibited by anti-apoptotic Bcl-2-like proteins. MPT might involve the formation of protein-permeable pores by oligomers of Bax and Bak (two pro-apoptotic proteins of the Bcl-2 family), as well as the transient or permanent opening of a variety of different channels, including those contained in the permeability transition pore complex (PTPC), such as the voltage-dependent anion channels (VDAC) in the outer membrane and the adenine-nucleotide translocase (ANT) in the inner membrane. In addition to PTPC-dependent mechanisms, recent findings suggest that apoptotic proteins such as cytochrome c can be released from the mitochondria by as yet
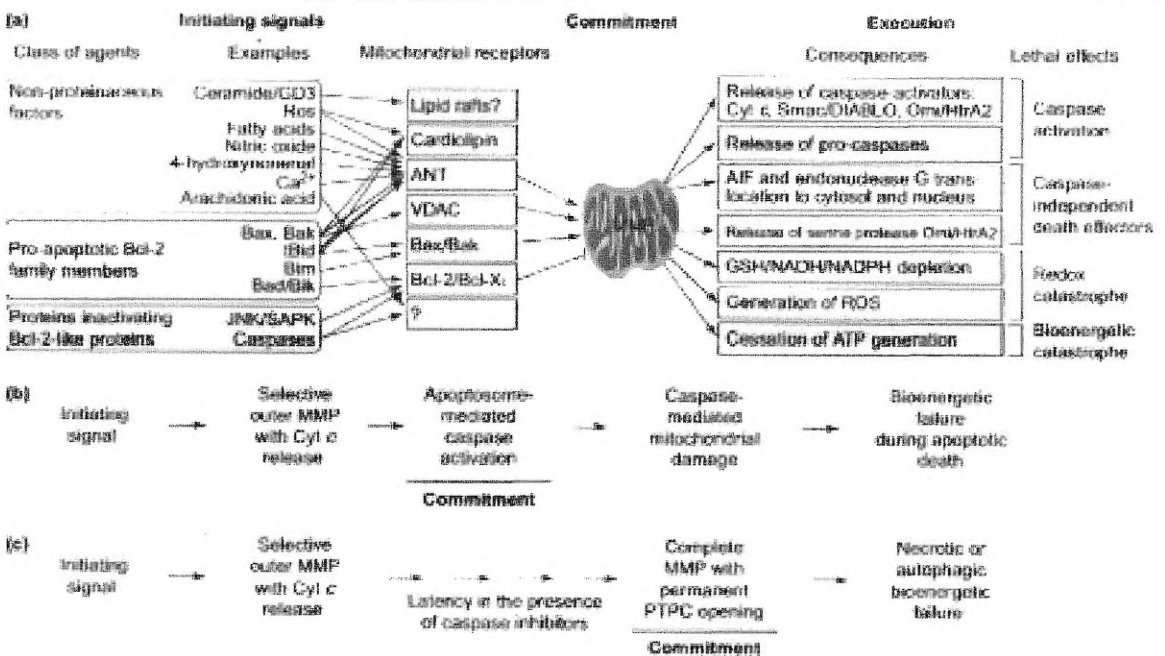

Fig.1. The importance of mitochondrial membrane permeabilization in apoptosis. Different apoptogenic molecules act on a variety of tenetively identified MPT regulator. MPT has several functional consequence resulting in cell death via both caspase-dependent and caspase-independent death effectors.

7

undetermined mechanisms that do not involve formation of PTPC. Furthermore, different K^+-selective channels in the inner membrane might control the volume of the mitochondrial matrix and ultimately the intactness of mitochondrial membranes. Moreover, inner-membrane uncoupling proteins (UCPs), which regulate the transmembrane proton gradient and the production of ROS and ATP, are increasingly being recognized for their roles in modulating cell death. Irrespective of the exact mechanism of MPT, it appears that this event can mark the 'point of no return' in the cell death process.

The mechanism of mitochondrial permeability transition (MPT).

Mitochondria are organelles with two well-defined compartments: the matrix, surrounded by the inner membrane (IM), and the intermembrane space, surrounded by the outer membrane (OM). The IM is folded into numerous christae, which greatly increases its surface area. It contains the protein complexes from the electron transport chain, the ATP synthase and the adenine nucleotide translocator (ANT). To function properly, the IM is almost impermeable to the various metabolites in physiological conditions (except for the those that have regulated transport mechanism), thereby allowing the respiratory chain to create an electrochemical gradient ($\Delta\Psi$). The $\Delta\Psi$ results from the respiration-driven, electron-transport-chain-mediated pumping of protons out of the inner membrane and is indispensable for driving the ATP synthase which phosphorylates ADP to ATP. ATP is then exported in exchange for ADP by the ANT. The OM in normal conditions is permeable to solutes up to about 5,000 Da. Thus, whereas the matrix space contains a highly selected set of small molecules, the intermembrane space is chemically equivalent to the cytosol with respect to low-molecular-weight solutes. The OM permeabilization involves the release of proteins which are normally confined to the intermembrane space, including cytochrome c, Smac/DIABLO, Omi/HtrA2 and AIF. The IM permeabilization may occur in a 'step-wise' manner (Green and Reed 1998; Bernardi 1999), with increasing permeability of solutes up to about 1,500 Da (Fig. 2.), and is

manifested as the dissipation of the proton gradient responsible for the trans-membrane

potential ($\Delta\Psi$), an extrusion of small solutes (such as calcium or glutation), or an influx of

water and sucrose (which, in sucrose-containing media, leads to large-amplitude swelling of
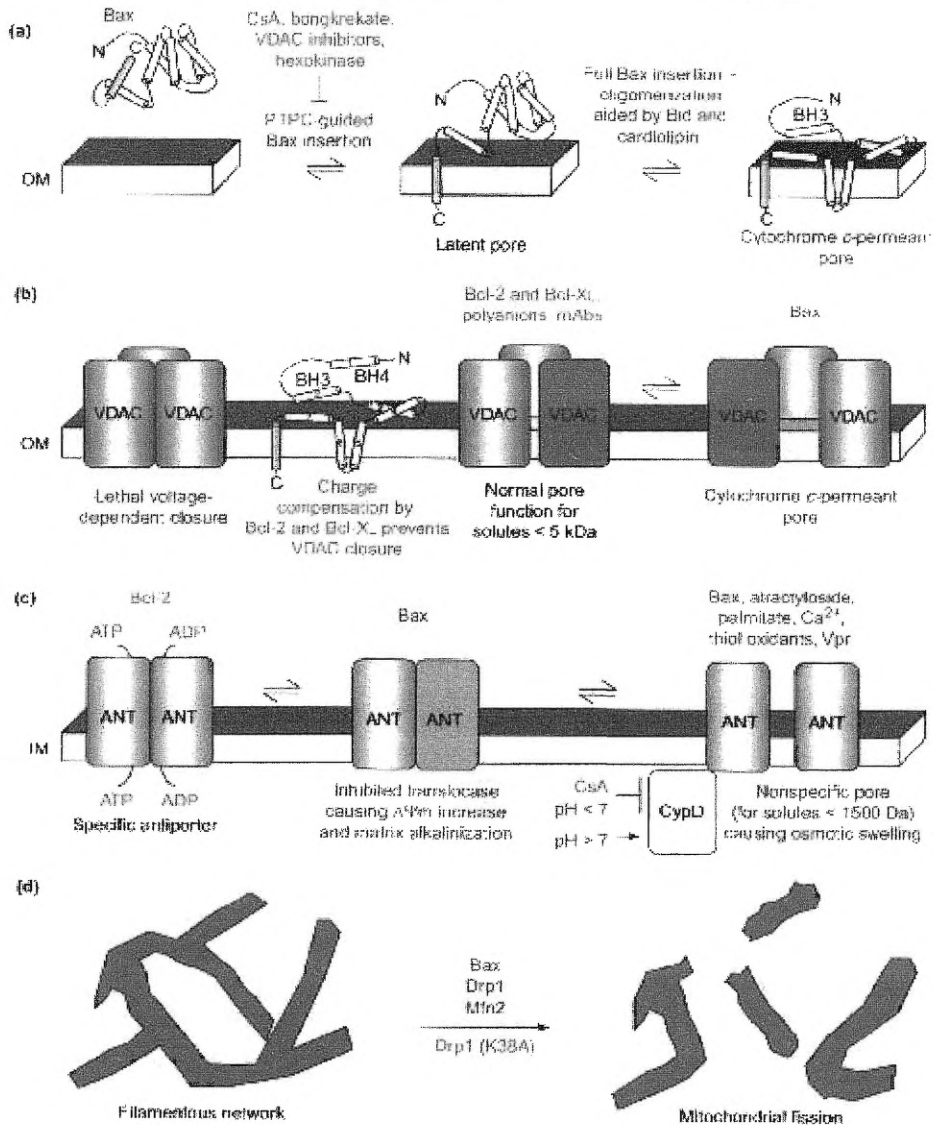
the matrix).

Fig. 2. Possible mechanisms of mitochondrial permeability transition (MPT). The precise mechanisms of MPT are still unsolved and might depend on the initiating stimulus. Inhibitors of permeabilization are denoted in red and inducers are in green. Adenine-nucleotide translocase (ANT), voltage-dependent anion channel (VDAC) and cyclophillin D (CypD), as well as Bcl-2-like proteins, might be organized in higher-order molecular complexes, such as the so-called permeability transition pore complex (PTPC).

9

The role of mitochondrial permeablity transition (MPT) in diseases.

Mitochondria in acute neuronal death.

Ischemic strokes and traumatic injuries to the brain and spinal cord are responsible for the prolonged disability or death of millions throughout the world. Studies of patient tissues and of animal models have shown, that mitochondria-mediated apoptosis is the mode of cell death of many neurons after an acute stroke or traumatic injury (Fiskum, 2000). Neurons are particularly sensitive to the oxygen and glucose deprivation that occurs during an ischemic stroke. Although neurons in the ischemic core die rapidly by necrosis, the majority of the neurons that die in the surrounding brain tissue (the penumbra) die by apoptosis. Several factors play a role in triggering MPT and neuronal apoptosis. Over-activation of receptors for the excitatory neurotransmitter, glutamate, under conditions of reduced energy availability results in excessive calcium accumulation ant the generation of ROS, both that can trigger MPT (Fig. 3.).
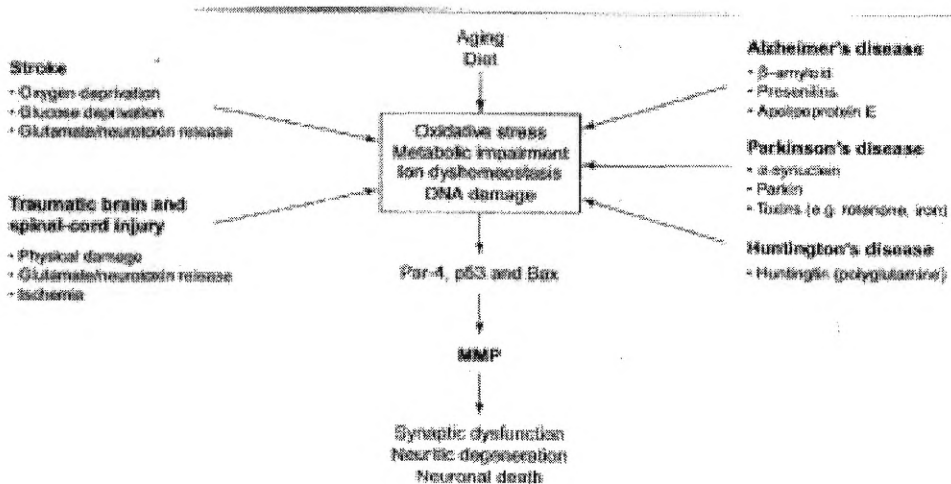

Fig. 3. The pivotal role of mitochondrial membrane permeabilization in neuronal death and chronic neurodegenerative disorders. In acute disorders neurons are deprived of oxygen and glucose, and are subjected to increased levels of neurotoxins released from damaged cells. In chronic disorders neuronal death is triggered by specific genetic mutations and/or environmental factors.

Mitochondria in neurodegenerative disease.

The prevalence of chronic age-related neurodegenerative disorders like Alzheimer's, Parkinson's and Huntington's disease is increasing rapidly. Cell cultures and animal models of these disorders, and studies of patients revealed that apoptosis involving MPT has a pivotal role in disease pathogenesis (Mattson, 2000). The factors that trigger apoptosis might differ among the neurodegenerative disorders (Fig. 3.), but each trigger appears to feed into a shared death cascade that involves increased oxidative stress and perturbed cellular energy and ion homeostasis. Stabilization of mitochondrial membranes by genetic manipulation of endogenous regulators of MPT or by treatment with pharmacological inhibitors of MPT suggest a necessary role for MPT in the pathogenesis of the neurodegenerative diseases.

Mitochondria in myocardial cell death.

MPT is crucial to both acute and chronic degenerative cardiac myocyte death (Borutaite and Brown, 2003). Apoptosis might represent an acute ischemia-induced phenomenon, and an important mechanism of progressive myocardiocyte loss and left-ventricular remodeling resulting from heart failure. Inhibitory studies, mostly performed on isolated hearts subjected to ischemia reperfusion, indicate that PTCP components as well as mitochondrial ATP-sensitive potassium (mitoK$_{ATP}$) channels play a major role in acute heart muscle cell death. Opening of the PTPC is likely to be caused by ROS and by an increase in cytosolic Ca^{2+} levels, and reportedly involves enhancement of the interaction between ANT and cyclophilin D.

MPT and cancer.

The defects in the regulation of apoptosis contribute to the development of cancer. Cancer cells almost invariably acquire mutations that allow them to evade the normal signals and mechanisms that cause apoptotic cell death. Indeed, it has been argued that resistance to apoptosis is a necessary, although insufficient, step for malignant progression. Thus, for

example, genetically modified mice that are compromised in their ability to engage one or more apoptotic pathway (and survive to adulthood) generally die prematurely of cancer. The induction of MPT in cancer cells by drugs therefore can be an effective method in the cancer therapy of the future.

Objectives

Numerous drugs used in human therapy exert toxic effects on tissues and cells. Since the mitochondria is involved the apoptotic cell death process, we analyzed the effects of well known toxic drugs on the mitochondrial functions.

Taxol is a widely used antitumor agent (Horowitz, 1992). It stabilizes tubulin dimers, thus interfering with microtubular disassembly (Schiff et al, 1979), and resulting in the arrest of cells in G_2-M phase of the cell cycle, followed by DNA fragmentation and morphological features of apoptosis. Paclitaxel has also been shown to activate Raf-1 and cause phosphorylation of Bcl-2 (Haldar et al., 1996; Ibrado et al., 1997), inactivating Bcl-2 and depriving it of forming heterodimers with the proapoptotic Bax (Haldar et al., 1995), hence leading to increased free intracellular Bax level. These effects of Taxol were exerted in the nM-µM concentration range ususally after a 2-24 h exposure to the drug, with a tendency of longer exposure times for lower concentrations (Torres and Horowitz, 1998). Effect of paclitaxel on the mitochondrial permeability transition pore was also suggested to be mediated through interaction with the cytoskeleton (Evtodienko et al., 1996). Despite numerous studies, mechanisms of mitochondrial effect of paclitaxel still remains to be elucidated. Therefore, we studied the direct mitochondrial effects of paclitaxel, namely, the induction of mitochondrial ROS production, the collapse of mitochondrial membrane potential and the opening of mitochondrial permeability pore, aiming to provide a novel molecular mechanism for the cytotoxicity of paclitaxel that can explain its toxic effect in slowly replicating and non dividing cells.

Amiodarone, a class III antiarrhythmic agent prolongs action potential duration which effect may involve blocking of β-adrenergic receptors, sodium channels and L-type calcium channels (Singh and Vaughan Williams, 1970). It is one of the most effective antiarrhythmic

drugs, and is frequently used in the clinical practice. However its administration is often limited by its toxic side effects, including pulmonary, liver and pancreas fibrosis, and thyroid dysfunction (Amico et al., 1984). The beneficial antiarrhythmic effect and the toxic effects on extracardiac tissues indicate a different sensitivity of the tissues toward amiodarone. However it has serious side effects limiting its clinical use. We analyzed if mitochondria plays a role in the beneficial cardiac and toxic extracardiac effects of amiodarone. and its major metabolite, N-desethylamiodarone. Conflicting reports appeared about the effect of the drug on cardiac functions in human studies (Remme and van Hoogenhuyze, 1990; Ellenbogen et al., 1985). Some reports presented beneficial effects of amiodarone during ischemia-reperfusion of perfused rat hearts (Karlson et al. 1990), whereas according to an other study, the drug improved hemodynamic parameters while it worsened the damages to the mitochondrial energy metabolism caused by ischemia-reperfusion (Moreau et al., 1999). The various results indicate that the molecular mechanism of the drug on cardiomyocyte function is poorly understood. In our study, we determined the effect of amiodarone on mitochondrial energy-metabolism during ischemia-reperfusion of Langendorff-perfused rat hearts by *in situ* ^{31}P-NMR spectroscopy. Assessing the direct effect of the drug on cardiac and extracardiac tissue, we determined the cytotoxicity of amiodarone on cells in culture. In an attempt to reveal the underlying mechanism of the drug in these paradigms, we studied its direct mitochondrial effects including induction of reactive oxygen species production, opening of PTP, and its effect on the mitochondrial respiration. We also compared the effect of amiodarone to other antiarrhythmic drug, and also to it's major metabolite, N-desethyl-amiodarone.

Materials and Methods.

Materials. Paclitaxel was from ICN Biomedicals Inc.; Taxol was from Bristol Myers Squibb; CsA was from Biomol Research Labs. Inc. ; rhodamine123 (Rh123), dihydrorhodamine123 (DRh123) and N-acetyl-8-dodecyl-3,7-dihydroxyphenoxazine (resorufin) were from Molecular Probes; amiodarone was from Chinoin Sanofi; all other compounds were from Sigma Chemical Co. unless otherwise stated.

Animals. Wistar rats kept under standardized conditions; tap water and rat chow were provided ad libitum. Animals were treated in compliance with approved institutional animal care guidelines.

Cell culture. PANC-1 human pancreatic epithelioid carcinoma cells, BRL 3A rat liver cells, HepG-2 human hepatocellular carcinoma, WRL 68 human liver cells, H9C2 mouse cardiomyocytes and Sp-2 mouse myeloma cells were from American Type Culture Collection. PANC-1, BRL-3A, HepG-2, WRL 68 and H9C2 cells were cultured in DMEM containing 1% antibiotic-antimycotic solution (Sigma) and 10 % FCS. Sp-2 cells were cultured in RPMI 1640 medium containing L-glutamin (2 mM), penicillin (100 U/ml), streptomycin (100 µg/ml) and 10 % FSC. Cells were passaged at intervals of 3 days.

Isolation of mitochondria. Rat liver and heart mitochondria were prepared according to standard protocol (Schneider and Hageboom, 1950). The only difference among the organs were in their homogenization; liver and kidney were squeezed through a liver press, while pooled heart tissue from 5 rats was minced with a blender. Brain mitochondria was prepared as described (Sims 1990). Isolation of mitochondria from HepG-2 and BRL 3A cells were performed exactly as described (Almeida and Medina, 1998). All isolated mitochondria were purified by Percoll gradient centrifugation (Sims 1990).

Mitochondrial oxygen consumption was assessed by a Clark electrode. The mitochondrial respiration was measured in the presence of different concentrations of amiodarone or desethylamiodarone. Before performing experiments, RCR (respiratory control ratio) values of the mitochondria were determined and were found to be in the range of 2.1 ± 0.4 and 3.7 ± 0.6 for the mitochondria from the heart or liver respectively (Elimandi et al., 1997; Garcia et al., 1997). State 3 and State 4 respiration as well as the respiratory control ratio and the ADP/O ratio were assessed from the original registration curve.

Mitochondrial permeability transition was monitored by following the accompanying large amplitude swelling via the decrease in absorbance at 540 nm (Cassarino et al., 1999) measured by a Perkin-Elmer fluorimeter in reflectance mode. Mitochondrial permeability transition was induced by the addition of 60 μM Ca^{2+} or of amiodarone at the indicated. Decrease of E_{540} and fluorescence intensity changes were detected for 20 min. The representative results demonstrated were selected from at least five independent experiments, each repeated three times, using mitochondria prepared from the same liver or pool of rat hearts respectively.

Enzymatic permeability transition assay. Measuring of citrate synthase (EC 4.1.3.7) and carnitine acyl transferase (EC 2.3.1.7) activity after the induction of permeability transition was performed as described (Korge and Weiss, 1999).

Alterations in the mitochondrial membrane potential following the induction of permeability transition was monitored by fluorescence of Rh123, released from the mitochondria and detected by a Perkin-Elmer fluorimeter at an excitation wavelength of 495 and an emission wavelength of 535 nm. Briefly, mitochondria at the concentration of 1 mg protein/ml were pre-incubated in the assay buffer containing 1 μM Rh123 and the tested compounds for 60 seconds. Alteration of the mitochondrial membrane potential ($\Delta\psi$) was induced by the addition of either 60 μM of Ca^{2+}, or amiodarone or desethylamiodarone at the

16

indicated concentrations. Changes of fluorescence intensity were detected for 4 min. The results are demonstrated by representative original registration curves from five independent experiments, each repeated three times using mitochondria prepared from the same liver or pool of rat hearts respectively

The determination of ROS-formation. ROS formation was detected as described (Varbiro et al., 2001) by the fluorescence of Rh123 formed by ROS-induced oxidation of the non-fluorescent DRh123 in situ at an excitation wavelength of 495 nm and an emission wavelength of 535 nm by a Perkin-Elmer fluorimeter (London, UK). The ROS-induced oxidation of N-acetyl-8-dodecyl-3,7-dihydroxyphenoxazine forms N-acetyl-8-dodecyl-resorufin (resorufin) which exhibits strong red fluorescence. This product is well retained in living cells and organelles by virtue of its lipophilic tail, making it possible to detect ROS production in the lipid phase. The method is the same as described above except for changing the excitation wavelength to 578 nm and the emission wavelength to 597 nm. ROS-formation was calculated from the slope of the registration curves

Detection of cytochrome c release *in vitro* was performed as described. Samples from the cuvette were taken prior to, and 3 minutes after the induction of the permeability transition, and centrifuged at 15000 X g for 15 minutes. Supernatants were analyzed for cytochrome c by Western blotting. Enhanced chemiluminescence labelling was used for the visualisation of the blots. Results are demonstrated by photomicrograph of a representative blot showing only the samples taken 3 minutes after the induction of the permeability transition.

Cell viability assay. PANC-1, BRL-3A, WRL 68 and H9C2 cells were seeded into 96-well plates at a starting density of 2.5 x 10^4 cell/well and cultured overnight. The following day, amiodarone at the indicated concentrations was added to the medium. Forty-eight hours later, 0.5 % of the water soluble mitochondrial dye, (3-(4,5-dimethylthiazol-2-yl]-2,5-diphenyl-tetrazolium bromide (MTT^+) was added. Incubation was continued for 3 more hours, the

medium was removed, and the water insoluble blue formasan dye formed stochiometrically from MTT$^+$ was solubilized by acidic isopropanol. Optical densities were determined by an ELISA reader (Anthos Labtech 2010) at 550 nm wavelength. All experiments were run in at least 4 parallels and repeated 3 times.

Oxygen consumption of cell lines H9C2, PANC-1 and BRL-3A were assessed by a Clark electrode (D'Aurelio et al., 2001,Beltran et al., 2002). The cells (1.5 x 10^7 cells per ml) were permeabilized by 50 µg/ml digitonin to enable the penetration of the substrates and the different concentrations amiodarone.

DNA electrophoresis. Sp-2 and H9C2 cells at a starting density of 6 x 10^6 /10 cm plate were cultured in the presence of different concentrations of amiodarone for 24h, then were collected. Cell viability was assessed by the trypan blue dye exclusion method. DNA fragmentation was monitored by gel electrophoresis as described before (Gorczyca et al., 1991). Electrophoresis was performed and DNA was visualized under UV light and photographed. Data presented as representative photomicrographs of at least three parallel experiments.

Demonstration of permeability transition in cultured cells. BRL 3A cells were seeded to glass coverslips (60 x 40 mm) at a starting density of 2500 cells/cm^2. The following day, CoverWell perfusion chambers were mounted on to the coverslips that allowed fast replacment of the medium on the cells. Cells were loaded with 1 µg/ml of Rh123 dissolved in culture medium for 30 min at 37 °C. After three washes 20 µM paclitaxel alone or with 2.5 µM CsA in KRH buffer containing 5 µg/ml propidium iodide (PI) was added. Incubation was continued under the microscope at room temperature, and fluorescent images were taken periodically.

The fluorescence of Rh123 and PI was monitored using a Bio-Rad MRC-1024ES laser scanning confocal attachment mounted on a Nikon Eclipse TE-300 inverted microscope. Cells

were excited with the 488 nm line of argon ion laser. Excitation light was passed through a dichroic mirror with a dividing wavelength of 527 nm preventing the exciting light to reach the detectors. The emitted fluorescent light was divided by a 565 nm dichroic mirror and was measured by separate photomultipliers through a 522/35 nm and a 680/32 nm band-pass filter. Laser intensity was attenuated by 99% in order to minimize photobleaching. Fluorescence was imaged with a Plan Apo 100x/1.4 oil-immersion objective. Confocal images were transferred to a Compaq Prosigna 300 workstation and were processed by using Bio-Rad's LaserSharp and Photoshop software packages. In this arrangement, green and red colour represents Rh123 and PI fluorescence respectively.

Heart Perfusion. Rats weighing 350 g were pretreated with amiodarone or desethylamiodarone exactly as described previously (Nokin et al, 1987). Hearts were perfused via the aorta as described before (Szabados et al., 1999). After a washout (non-recirculating period of 15 min), hearts were perfused under normoxic conditions for 10 minutes; the flow was subsequently discontinued for 30 minutes by inflating a balloon (ischemia), which was followed by 15 minutes of reperfusion. Levels of high-energy phosphate intermediates were monitored in the magnet of a ^{31}P NMR spectroscope during the entire perfusion.

NMR Spectroscopy. NMR spectra were recorded with a Varian ^{UNITY}INOVA 400 WB instrument as described (Halmosi et al., 2000). Data were acquired from 5 independent experiment for sham-operated and amiodarone-treated groups each.

Western blot analysis of AIF. Myocardial specimens were snap-frozen immediately after surgical removal or at the end of the Lagendorff-perfusion experiment and stored at -80 °C until analyzed. Frozen heart muscle samples were mechanically homogenized in liquid nitrogen and the nuclear fraction was prepared as described (Schmitt et al., 2002). Equal amounts of nuclear extracts were separated by sodium dodecyl sulfate–polyacrylamide gel electrophoresis (12% gel) and then transferred to a nitrocellulose filter. Membranes were

blocked using 5% dry milk. The blot was probed with monoclonal antibodies against AIF overnight at the temperature of 4°C. The antigen–antibody complex was visualized on an X-ray film using secondary antibodies linked to horseradish peroxidase and a chemiluminescence kit. Results are demonstrated by photomicrograph of a representative blot.

Statistical analysis. Data were presented as means ± S.E.M. For multiple comparisons of groups ANOVA was used. Statistical difference between groups was established by paired or unpaired Student's *t* test, with Bonferroni correction.

Results.

Paclitaxel induces MPT and dissipation of $\Delta\Psi$ in isolated liver mitochondria. In a concentration dependent manner, paclitaxel induced swelling in isolated liver mitochondrion (Fig. 4.), in the presence of low concentration of Ca^{2+} (2.5 μM). This amount of Ca^{2+} did not induce permeability transition by itself. Paclitaxel at a concentration of 20 μM caused maximal swelling of mitochondria (same as induced by 150 μM Ca^{2+}) that was prevented
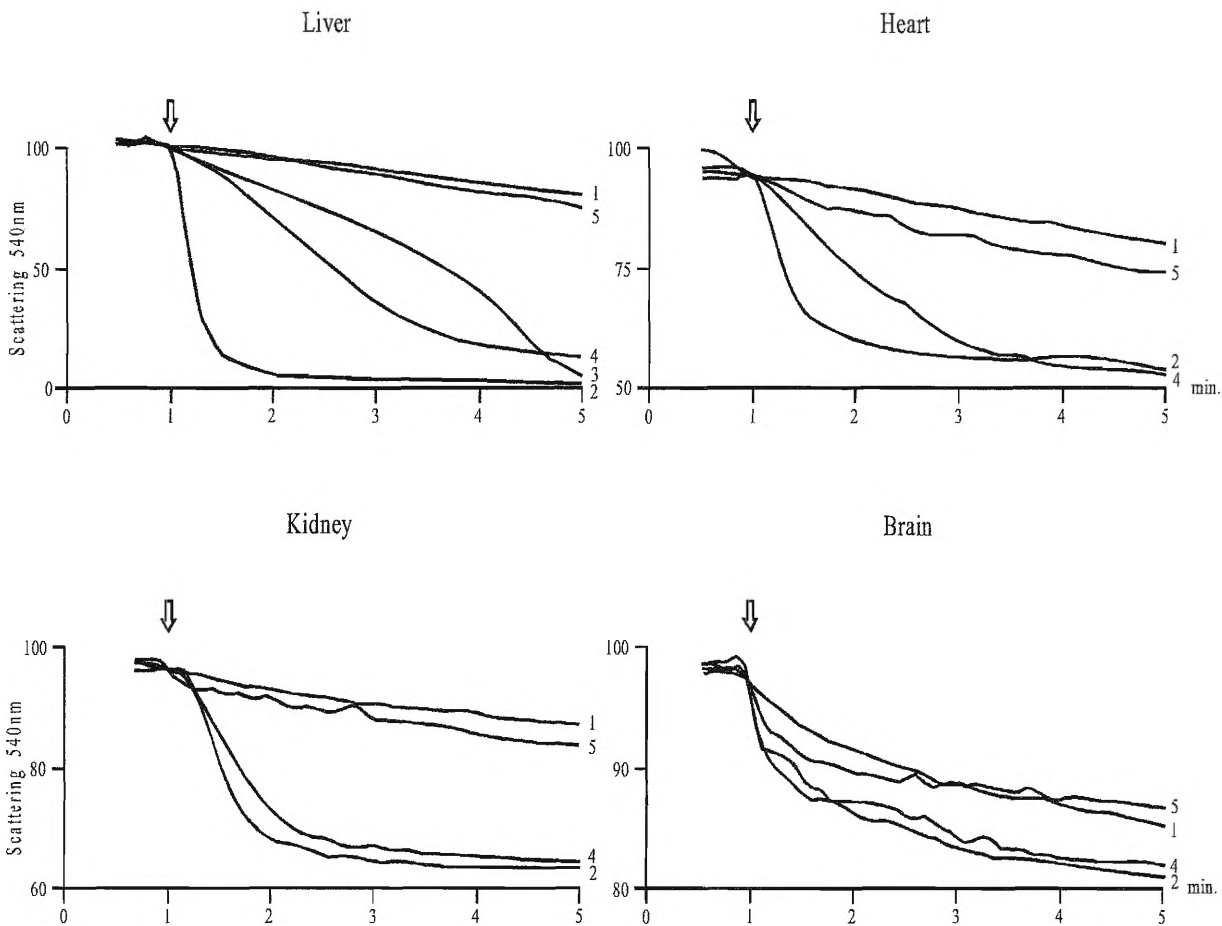
Fig. 4. Permeability transition induced by different concentration of paclitaxel and 150 μM Ca^{2+} in isolated rat liver, heart, kidney and brain mitochondria. Mitochondria in the presence or absence of CsA was incubated at room temperature in permeability transition-buffer as described in Materials and Methods. Permeability transition-inducing agents were added at arrow. Results are demonstrated by representative original registration curves for at least five independent experiments. Line 1: no agent added; line 2: 150 μM Ca^{2+}; line 3: 10 μM paclitaxel; line 4: 20 μM paclitaxel; line 5: 20 μM paclitaxel + 2.5 μM CsA.

21

completely by 2.5 μM CsA. Twenty μM paclitaxel caused the dissipation of Δψ (Fig. 5.), as

detected by the release of the membrane potential sensitive dye, Rh123 from liver

mitochondria following the induction of permeability transition. Dissipation of ΔΨ was

inhibited by 2.5 μM CsA. The opening of the permeability transition pore allows the entering

of substrates (such as acetyl-coenzyme A) that are otherwise excluded by the inner

mitochondrial membrane into the mitochondrial matrix. It enabled us to demonstrate the

opening of the permeability pore by a simple enzyme assay. Citrate synthase and carnitine

acyltransferase activity become measurable using externally added acetyl-coenzyme A after

Fig. 5. Changes in ΔΨ induced by 20 μM of paclitaxel and 150 μM Ca^{2+} in isolated rat liver, heart, kidney and brain mitochondria. Mitochondria in the presence or absence of CsA was incubated at room temperature in permeability transition-buffer as described in Materials and Methods. Permeability transition-inducing agents were added at arrow. Results are demonstrated by representative original registration curves for at least five independent experiments. Line 1: no agent added; line 2: 150 μM Ca^{2+}; line 3: 20 μM paclitaxel; line 4: 20 μM paclitaxel + 2.5 μM CsA.

the addition of either 150 μM Ca^{2+} or 20 μM paclitaxel showing the opening of the permeability pore. This effect was inhibited by 2.5 μM CsA. Release of cytochrome c from the mitochondrial intermembrane space following permeability transition induced by either 150 μM Ca^{2+} or by 20 μM paclitaxel was detected by Western blotting. Cytochrome c release was inhibited in both cases by 2.5 μM CsA.

Paclitaxel induces MPT and dissipation of $\Delta\Psi$ of mitochondria isolated in different tissues and cultured cells. The degree and slope of the swelling differed greatly among the different tissues, with the highest value for liver, a lower value for kidney and heart, a value close to the detection limit for brain and a swelling below detection limit for the cell lines (Fig 4.). There were differences in the degree and slope of the Rh123-release among the different tissues similar as in the case of swelling (Fig. 5.). However, measuring of Rh123-release was much more sensitive than of swelling, so even for cell lines, the CsA-sensitivity of the Rh123-release induced by either 20 μM paclitaxel or 150 μM Ca^{2+} could be established.

Effect of amiodarone and desethylamiodarone on Ca^{2+}-induced MPT in isolated rat liver mitochondria. In isolated liver mitochondria, the swelling induced by 60 μM of Ca^{2+} was completely inhibited by 2.5 μM of CsA or by 1 μM of FCCP (data not shown). Depending on its concentration, amiodarone had a biphasic effect on mitochondrial swelling (Fig. 6.). Up to the concentration of 10 μM, amiodarone inhibited the rapid swelling induced by Ca^{2+} in a concentration dependent manner with the IC_{50} of 3.9 ± 0.8 μM. The most pronounced inhibitory effect of amiodarone on the swelling induced by 60 μM of Ca^{2+} was at the concentration of 10 μM. At higher concentrations, amiodarone proved to be less effective in delaying the Ca^{2+}-induced swelling. In contrast to amiodarone, desethylamiodarone did not show any inhibitory effect on the mitochondrial permeability transition induced by 60 μM of Ca^{2+} up to the concentration of 10 μM (Fig. 6.).

At concentrations above 10 μM, amiodarone induced mitochondrial swelling by its own (Fig. 7.), that was not inhibited by 2.5 μM of CsA. In contrast to 30 μM of amiodarone which developed swelling with a rate significantly slower than that of the Ca^{2+}-induced swelling, desethylamiodarone, at the concentration of 30 μM induced swelling with a rate
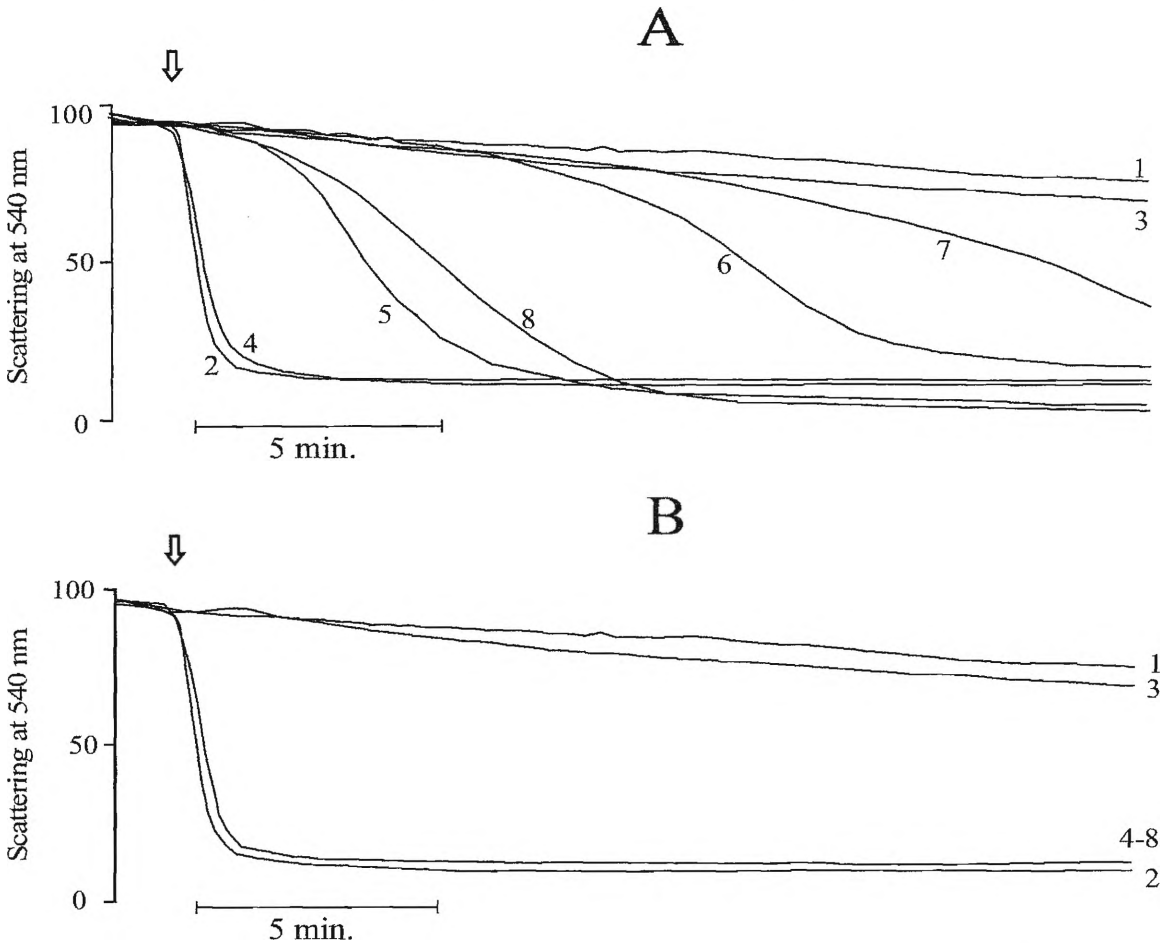

Fig. 6. The effect of amiodarone or desethylamiodarone on Ca^{2+}-induced mitochondrial swelling. Mitochondrial swelling was demonstrated by monitoring E_{540} in isolated rat liver mitochondria. Amiodarone (Ad) at the indicated concentration or 2.5 μM cyclosporin A (CsA) was present throughout the experiment(A). Alternatively desethylamiodarone (Dea) at the indicated concentration or 2.5 μM cyclosporin A (CsA) was present throughout the experiment (B). The mitochondrial permeability transition (swelling) was induced by adding 60 μM Ca^{2+} at arrow
(A) Line 1: baseline swelling (no agent); line 2: 60 μM Ca^{2+}-induced swelling (no Ad or CsA); line 3: CsA; line 4: 1 μM Ad; line 5: 2.5 μM Ad; line 6: 5 μM Ad; line 7: 10 μM Ad; line 8: 20 μM Ad.
(B) Line 1: baseline swelling (no agent): line 2: 60 μM Ca^{2+}-induced swelling (no Dea or CsA); line 3: CsA; line 4: 1 μM Dea; line 5: 2.5 μM Dea; line 6: 5 μM Dea; line 7: 10 μM Dea; line 8: 20 μM Dea.

similar to that of the Ca^{2+}-induced one. The swelling induced by desethylamiodarone was not inhibited by 2.5 µM of CsA (Fig. 7.). The effect of amiodarone or desethylamiodarone on isolated rat heart mitochondria was basically the same, as on liver mitochondria
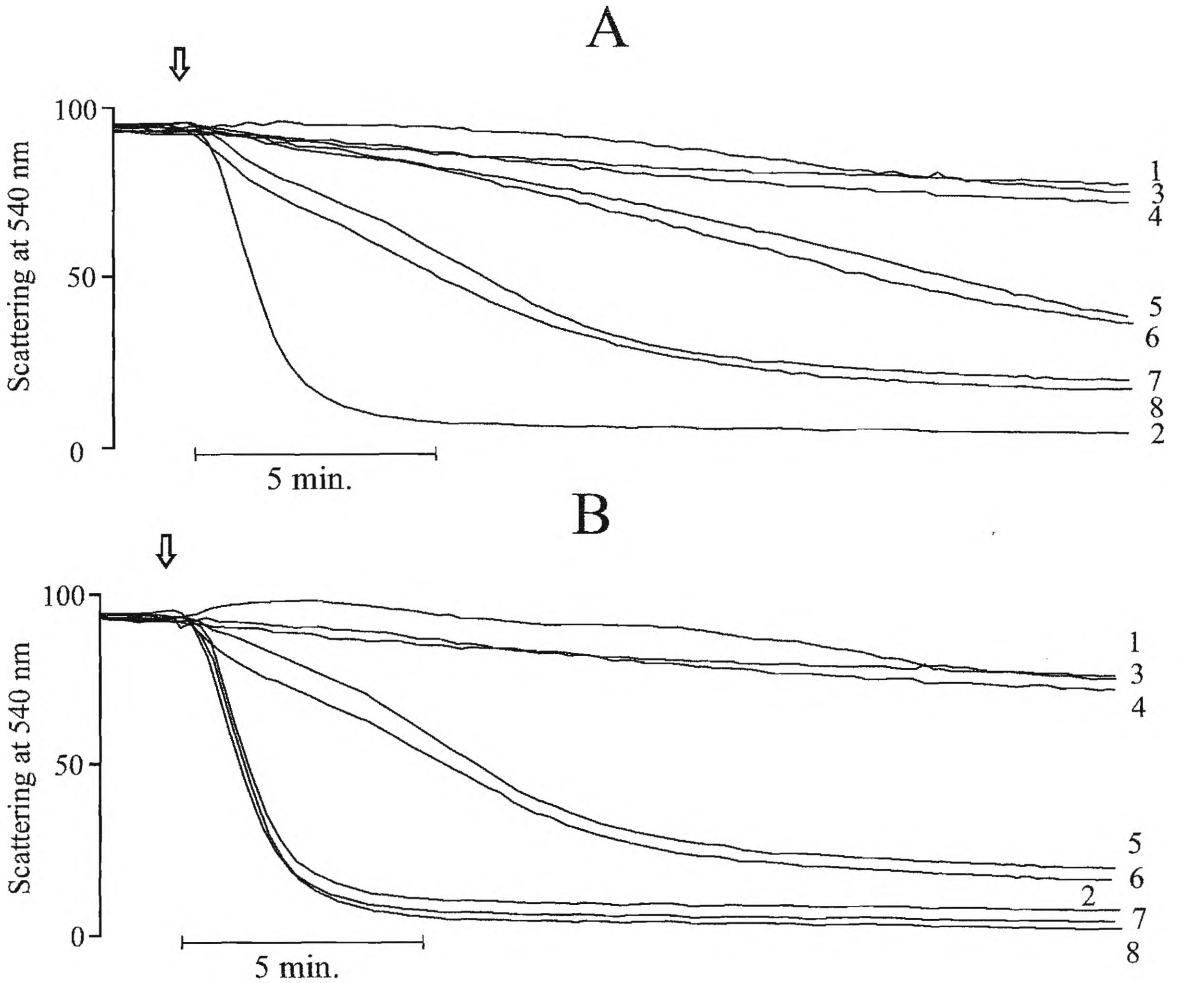

Fig. 7. The mitochondrial swelling induced by amiodarone or desethylamiodarone. Mitochondrial swelling was demonstrated by monitoring E_{540} in isolated rat liver mitochondria. Cyclosporin A (CsA), at the concentration of 2.5 µM, where indicated, was present throughout the experiment. Swelling was induced by adding amiodarone (Ad) at the indicated concentration (A) or desethylamiodarone (Dea) at the indicated concentration (B), or 60 µM Ca^{2+} at the arrow.
(A) Line 1: baseline swelling (no agent); line 2: 60 µM Ca^{2+}-induced swelling (no Ad or CsA); line 3: 10 µM Ad; line 4: 10 µM Ad + CsA; line 5: 20 µM Ad; line 6: 20 µM Ad+ CsA; line 7: 30 µM Ad; line 8: 30 µM Ad + CsA.
(B) Line 1: baseline swelling (no agent); line 2: 60 µM Ca^{2+}-induced swelling (no Dea or CsA); line 3: 10 µM Dea; line 4: 10 µM Dea + CsA; line 5: 20 µM Dea; line 6: 20 µM Dea+ CsA; line 7: 30 µM Dea; line 8: 30 µM Dea + CsA.

The opening of the permeability transition pore allows the entering of substrates (such as acetyl-coenzyme A) that are otherwise excluded by the inner mitochondrial membrane into the mitochondrial matrix. It enabled us to demonstrate the opening of the permeability pore by a simple enzyme assay. Citrate synthase and carnitine acyltransferase activity become measurable using externally added acetyl-coenzyme A after the addition of 60 μM of Ca^2 showing the opening of the permeability pore. This effect was also delayed by 10 μM of amiodarone.

Effect of amiodarone and desethylamiodarone on dissipation of ΔΨ in isolated liver mitochondria. Sixty μM Ca^{2+} caused the dissipation of ΔΨ, as detected by the release of the membrane potential sensitive dye, Rh123, from isolated liver mitochondria (Fig. 8.). When the mitochondrial membrane was depolarized by Ca^{2+} in the presence of 2.5 μM CsA, after a transient depolarization lasting for about a minute, ΔΨ returned to the value identical to the one before the addition of Ca^{2+}. Ten μM of amiodarone depolarized the mitochondrial membrane in a similar extent as did the 60 μM of Ca^{2+}, however, its depolarizing effect was not influenced at all by 2.5 μM of CsA. Amiodarone caused a concentration dependent release of Rh123 from liver mitochondria with a calculated EC_{50} value of 4.2 ± 0.7 μM. In contrast to this, desethylamiodarone, up to the concentration of 10 μM did not induce the dissipation of ΔΨ. However, desethylamiodarone at the concentration of 20 μM caused Rh123 release from the isolated mitochondria as did 20 μM of amiodarone, 60 μM of Ca^{2+}, or as did 1 μM of FCCP. The calculated EC_{50} value for desethylamiodarone was 16.3 ± 2.3 μM. The depolarizing effect of 20 μM of desethylamiodarone was not influenced at all by 2.5 μM of CsA.
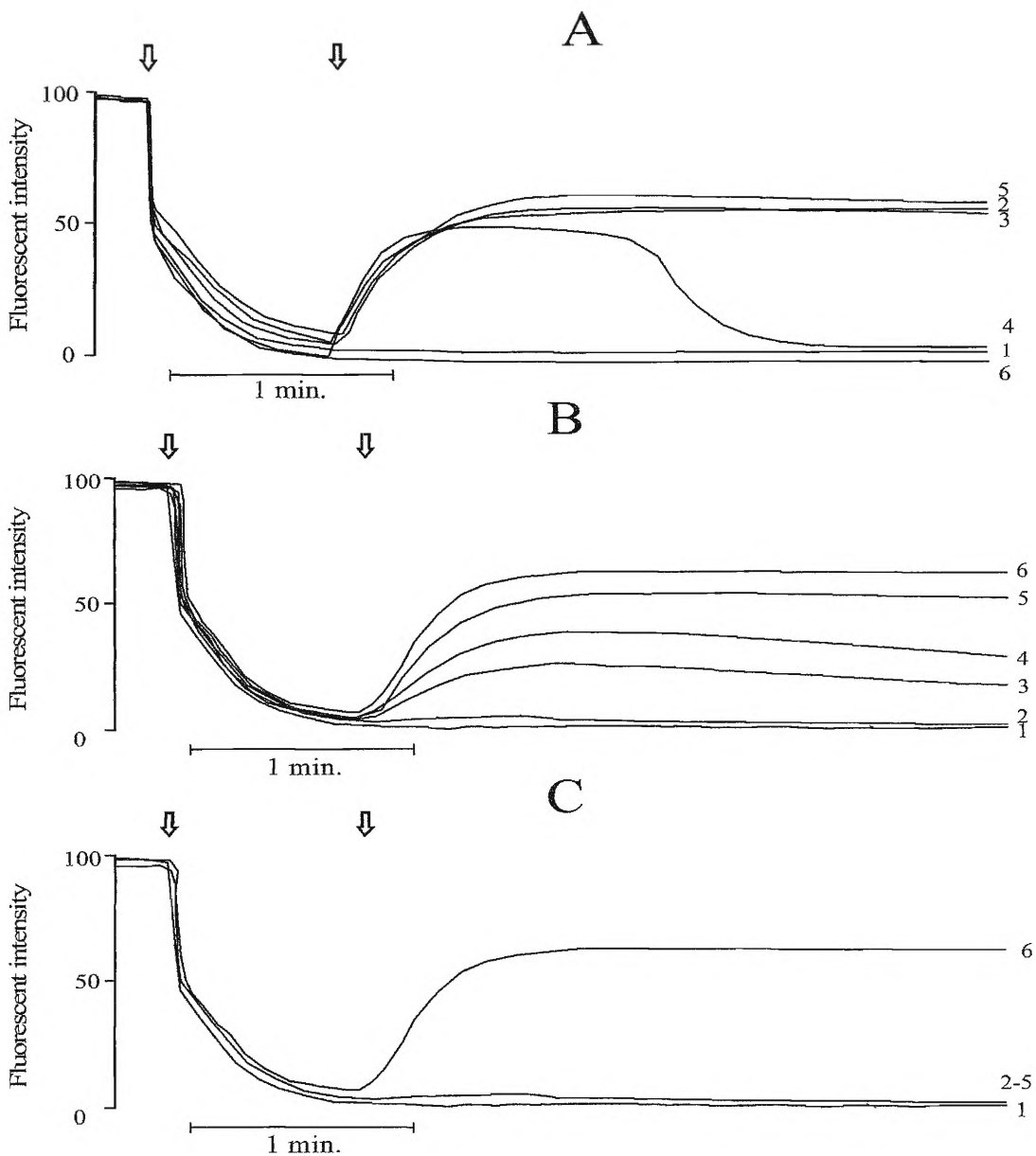
Fig. 8. Effect of amiodarone or desethylamiodarone on the mitochondrial membrane potential in isolated mitochondria. Membrane potential was monitored by measuring the fluorescence intensity of the cationic fluorescent dye rhodamine 123. Isolated rat liver mitochondria, added at the first arrow, takes up the dye in a voltage dependent manner and quenches its fluorescence. Amiodarone (Ad), desethylamiodarone (Dea) at the concentrations indicated or 60 µM Ca^{2+} (either added at second arrow) induces depolarization resulting in release of the dye and increase of the fluorescence intensity. (A) Line 1: no agent; line 2: Ca^{2+}; line 3: 10 µM Ad; line 4: Ca^{2+} + 2.5 µM CsA ; line 5: 10 µM Ad + 2.5 µM CsA; line 6: 10 µM Dea. (B) Line 1: no agent; line 2: 1 µM Ad; line 3: 2.5 µM Ad; line 4: 5 µM Ad; line 5: 10 µM Ad; line 6: 20 µM Ad (C) Line 1: no agent; line 2: 1 µM Dea; line 3: 2.5 µM Dea; line 4: 5 µM Dea; line 5: 10 µM Dea; line 6: 20 µM Dea.

27

Paclitaxel induces dissipation of ΔΨ in cell line. Confocal microscopy was used to monitor the changes in Rh123 and PI fluorescence images of BRL-3A cells (Fig. 9.). The cationic dye, Rh123 is retained by the mitochondria and shows green fluorescence image of the mitochondria when $\Delta\psi$ is intact, but is released into the cytosol and shows a weak background fluorescence when $\Delta\psi$ is disrupted in consequence to permeability transition. On the other hand, PI is excluded by intact cell membranes, but shows red fluorescent image of the nucleus when cellular energy charge drops to zero or the integrity of the cell membrane is damaged. Representative fluorescent images taken 45 minutes after the addition of paclitaxel
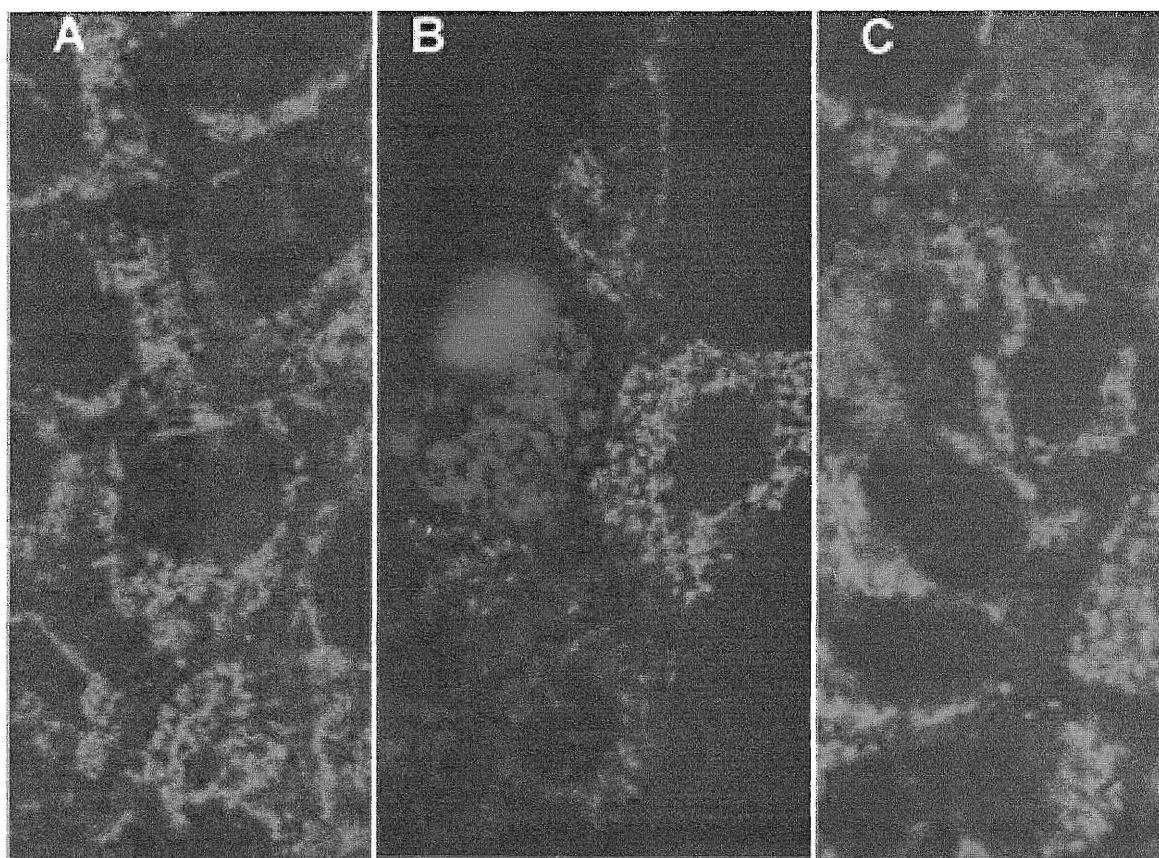

Fig. 9. Demonstration of permeability transition in BRL-3A cell line. Confocal fluorescent microscopy images of Rh123 (green) and PI (red) fluorescence were taken periodically. Cells cultured on coverslips were loaded with Rh123, washed, and incubated in medium containing 5 µg/ml PI in the absence or the presence of 20 µM paclitaxel together with or without 2.5 µM CsA as described in Methods. Representative double-fluorescence photos taken after 45 min of incubation are presented. A: no agent; B: 20 µM paclitaxel; C: 20 µM paclitaxel+2.5 µM CsA.

and CsA demonstrate the effect of these drugs on the cells. Green fluorescent dots of approximately the same intensity representing mitochondria were seen in each control cell. This pattern of uniform fluorescent intensity was maintained in control cells for several hours. When the cells were incubated for about 35 minutes in the presence of 20 µM paclitaxel, mitochondria in the cells started to undergo permeability transition which process was completed in 20 minutes indicated by a complete disappearance of green fluorescence. We demonstrated an intermediate state, when the green fluorescent intensity was decreased in some cells, completely disappeared in other cells and red PI fluorescence of a nucleus appeared in a cell indicating that permeability transition took place in the mitochondria of some cells as a consequence of 45 min incubation with 20 µM paclitaxel. CsA at a concentration of 2.5 µM inhibited the permeability transition-inducing effect of paclitaxel as revealed by fluorescent images identical to control.

Paclitaxel induces ROS formation in isolated rat liver mitochondria. Since ROS formation can induce the mitochondrial permeability transition, we studied the effect of paclitaxel on ROS production in isolated, Percoll gradient-purified rat liver mitochondria. ROS formation was measured by monitoring the green or red fluorescence of Rh123 or resorufin oxidized by the ROS from non-fluorescent DRh123 or N-acetyl-8-dodecyl-3,7-dihydroxyphenoxazine *in situ*, respecively (Fig. 10.). By virtue of its dodecyl group, resorufin was localized in membranous regions and detected ROS formation in lipid phase while Rh123 reflected to ROS levels in aqueous phase. Paclitaxel induced ROS-formation in isolated liver mitochondria in a concentration dependent manner. By using both dyes, we compared the ROS-formation induced by paclitaxel to that of 50 mM H_2O_2. A much more intense ROS-formation was detected by resorufin (61 ± 6.4 % that of 50 mM H_2O_2) than by Rh123 (21 ± 4.7 % that of 50 mM H_2O_2). When detected by Rh123, ROS formation induced by paclitaxel could be attenuated by 1 mM lipoamide, 1 mM ascorbic acid and in a smaller extent by 100

μM tocopherol, however, not by 1 mM N-acetyl-L-cysteine. ROS formation induced by paclitaxel was decreased by 1 mM lipoamide, 100 μM tocopherol and in a smaller extent by 1
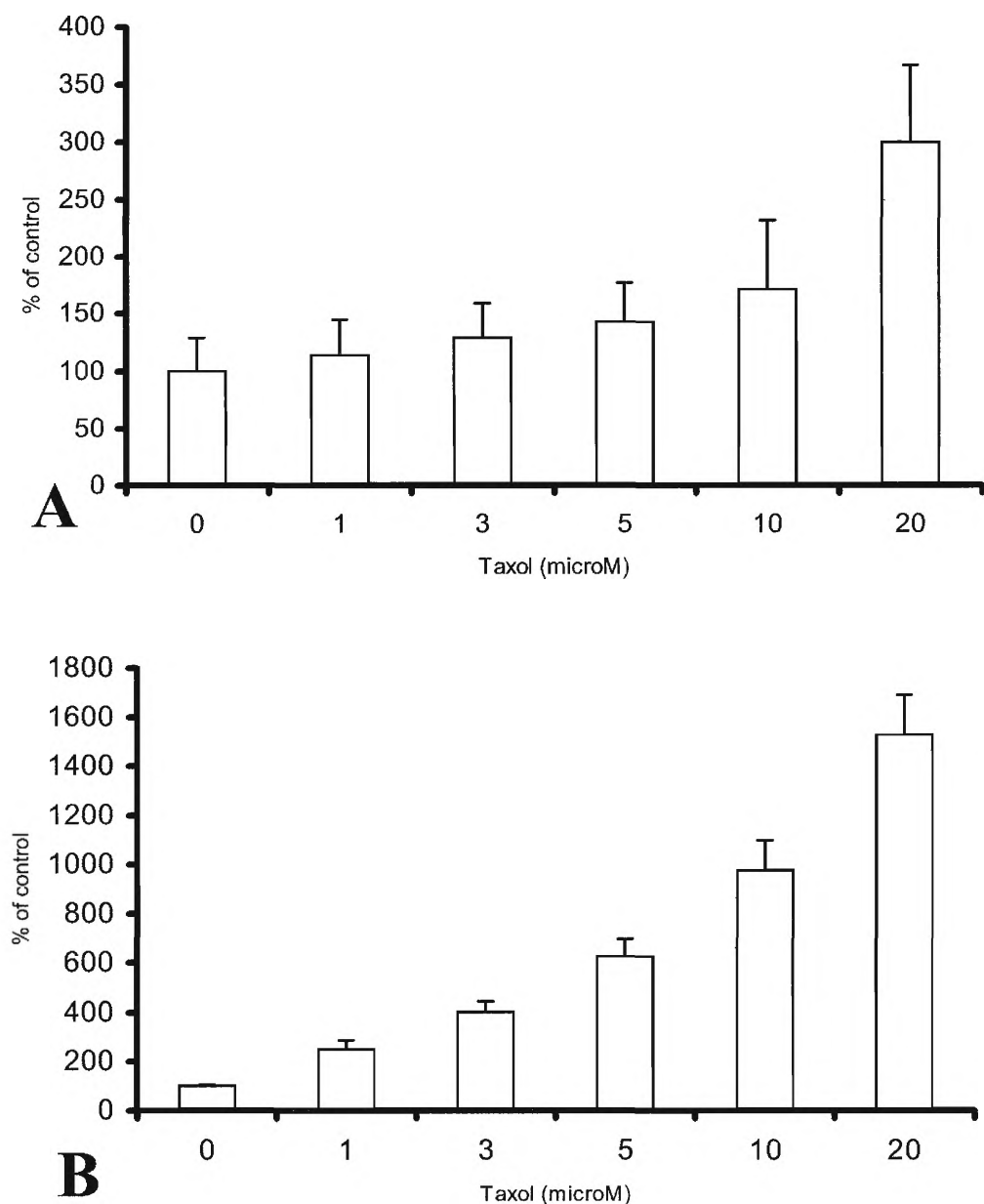

Fig. 10. ROS-formation in isolated mitochondria. Increase of fluorescence intensities of resorufin (A) and Rh123 (B) oxidized from non-fluorescent N-acetyl-8-dodecyl-3,7-dihydroxyphenoxazine and DHRh123 by ROS was measured as described in Materials and Methods. Resorufin and Rh123 fluorescence reflected to the paclitaxel induced ROS formattion in the aquous and the lipid phase respectively. Results were calculated from the slope of the original registration curves (fluorescent intensity vs. time) and expressed as % of the ROS-formation in the absence of paclitaxel. Values are mean ± S.E.M. of at least 5 independent experiments.

mM N-acetyl-L-cysteine, however, not by 1 mM ascorbic acid when detected by resorufin. Selective inhibitors of the respiratory complexes caused a transient fast increase of the mitochondrial ROS formation followed by a plateau where the rate of ROS formation was the same as before the addition of the given substance. When added on this plateau, paclitaxel induced ROS formation with a time-course similar to that observed in the absence of the inhibitors of the respiratory chain. However, KCN and other inhibitors of cytochrome oxidase, azide and NO, inhibited the paclitaxel-induced ROS production. Ca^{2+} at the concentration of 150 µM did not induce ROS formation, furthermore, the ROS formation induced by either 50 µM paclitaxel or 50 mM H_2O_2 could not be inhibited by 2.5 µM CsA.

The effect of amiodarone and desethylamiodarone on ROS formation in isolated rat mitochondria. Up to the concentration of 100 µM, amiodarone and desethylamiodarone did not induce ROS formation in mitochondria isolated from either liver or heart as detected by Rh123 or resorufin.

Effect of paclitaxel on mitochondrial oxygen consumption. Since inhibitors of the respiratory chain caused a transient ROS formation, we checked whether paclitaxel had inhibitory effect on mitochondrial respiration. Oxygen consumption was measured by using a Clark electrode in isolated rat liver mitochondria. Paclitaxel up to the concentration of 20 µM either alone, or in combination with up to 500 µM Ca^{2+} did not decrease the oxygen consumption supported by either succinate, or pyruvate under our experimental conditions.

Effect of amiodarone and desethylamiodarone on the mitochondrial oxygen consumption. The oxygen consumption of isolated mitochondria (state 4 respiration) was measured by a Clark electrode, with 10 mM pyruvate (Complex I supported respiration) or 10 mM succinate in the presence of 1 µM rotenone (Complex II supported respiration) exposed to different concentrations of amiodarone or desethylamiodarone (Fig. 11). In isolated rat heart mitochondria, at low concentrations, amiodarone did not have a significant effect either on

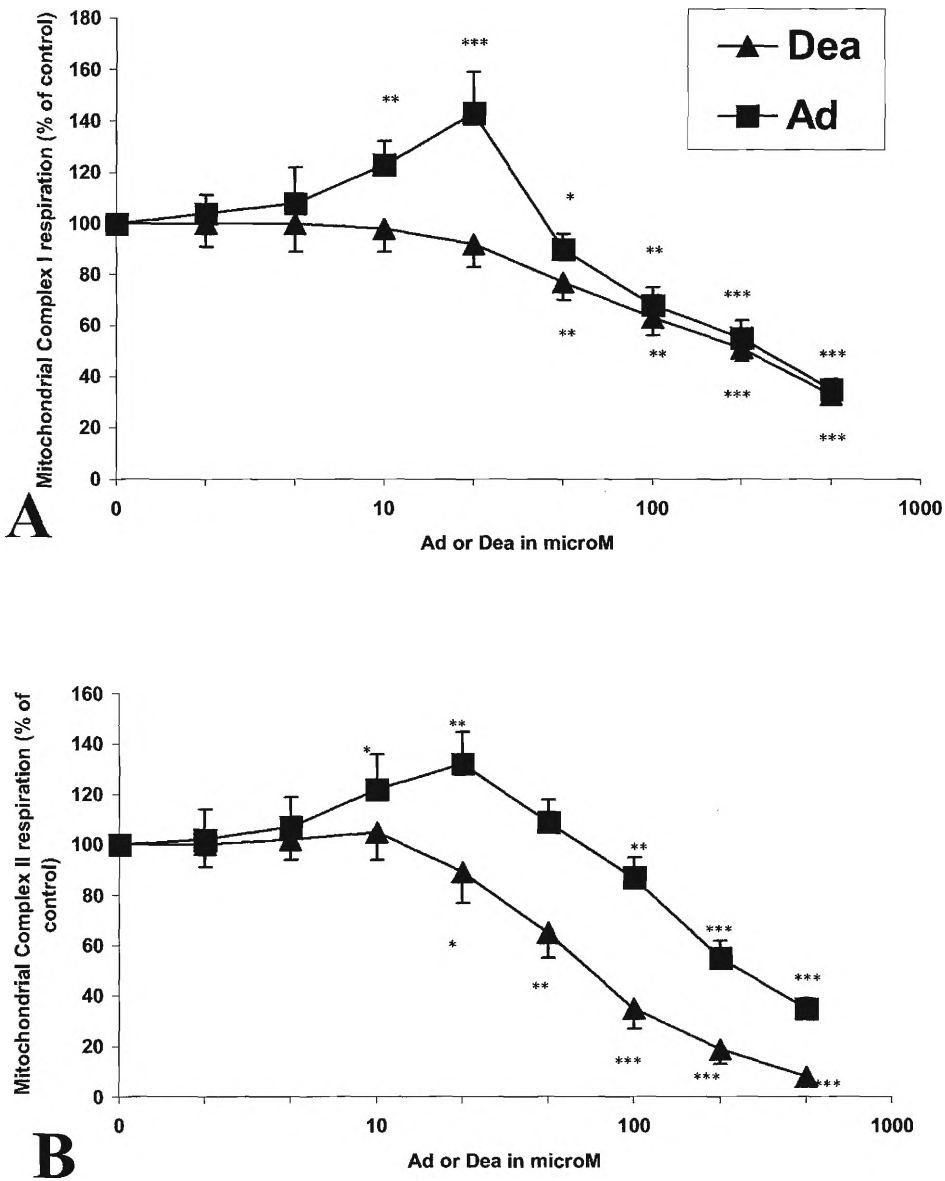Complex I or on Complex II supported respiration, as compared to the control. In an

Fig. 11. The effect of amiodarone and desethylamiodarone on mitochondrial oxygen consumption. Mitochondrial respiration was measured by a Clark electrode and was supported with either 10 mM pyruvate (Complex I respiration) or 10 mM succinate (Complex II respiration) in the presence of different concentrations of amiodarone or desethylamiodarone. Data represents average ± S.E.M. of three independent experiments repeated twice using mitochondria prepared from the same heart samples. Note that the concentration axis is logarithmic. *, significant difference (p < 0.05; mean ± S.E.M., paired *t* test); **, significant difference (p < 0.01; mean ± S.E.M., paired *t* test); ***, significant difference (p < 0.001; mean ± S.E.M., paired *t* test) of amiodarone or desethylamiodarone from control.

intermediate concentration range amiodarone increased both the Complex I- and Complex II-supported oxygen consumption indicating an uncoupling effect, while, the drug gradually inhibited respiration at higher concentrations.

Desethylamiodarone did not have any significant effect on the mitochondrial oxygen consumption at low concentrations of up to 10 μM. Above this concentration it gradually inhibited the respiration supported by succinate and in the concentration above 30 μM the respiration supported by pyruvate, without presenting an uncoupling effect, as indicated by the absence of the stimulation of both Complex I- and Complex II-supported respiration in the concentration range of 6 to 30 μM. Above 30 μM, desethylamiodarone inhibited Complex I supported respiration, similarly to that observed with equimolar concentrations of amiodarone. However, above the concentration of 30 μM, desethylamiodarone presented a significantly stronger inhibition ($p < 0.01$) on Complex II supported respiration, than the one observed with equimolar concentrations of amiodarone. The effect of amiodarone or desethylamiodarone on isolated rat liver mitochondria was basically the same.

Amiodarone induces internucleosomal fragmentation of genomic DNA. Following exposure of Sp-2 cells to different concentrations of amiodarone for 24 h, internucleosomal DNA fragmentation and the morphological features of apoptosis were detected from the concentration of 1 μM or higher. However, in H9C2 cells no DNA-laddering was observed in the presence of amiodarone up to the concentration of 30 μM (Fig. 12.).

Effect of amiodarone and desethylamiodarone on the viability of cultured cell lines. Viability of H9C2, BRL-3A, WRL-68 and PANC-1 cells exposed to different concentrations of amiodarone or desethylamiodarone for 48h were assessed by the MTT$^+$ method (Fig. 13). In all cell lines desethylamiodarone proved to be more toxic than amiodarone in a specific concentration range. This concentration range seemed to be variable in the different cell lines. The significant difference ($p < 0.001$) between the toxicity of amiodarone and

desethylamiodarone observed in H9C2 cardiomyocytes was in a concentration range between 10 to 60 μM. In the normal rat (BRL-3A) and human (WRL-68) liver cell lines the significant difference (p < 0.001 and p < 0.01 respectively) between the toxicity of the drugs appeared in a lower concentration range between 3 to 20 μM. In PANC-1 human pancreatic epithelioid carcinoma cells, significant difference (p < 0.01) between the toxicity of amiodarone and desethylamiodarone was observed in a concentration range of 20 to 80 μM as revealed by the viability data. The various cell lines presented different sensitivity towards the toxicity of amiodarone or desethylamiodarone. The drugs were shown to be the least toxic in H9C2 cardiomyocyte cells. BRL-3A and WRL-68 hepatocytes were much more sensitive to amiodarone or desethylamiodarone toxicity than the PANC-1 human pancreatic epithelioid carcinoma cells, however, BRL-3A and WRL-68 were normal, while PANC-1 was a cancer cell line.
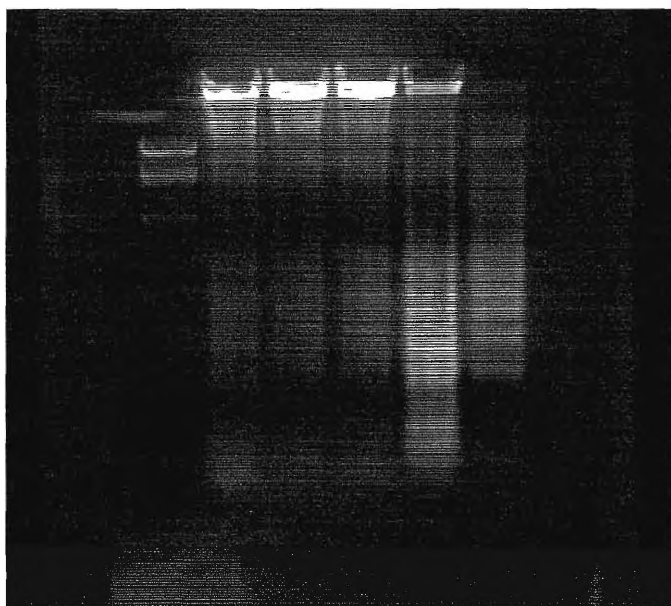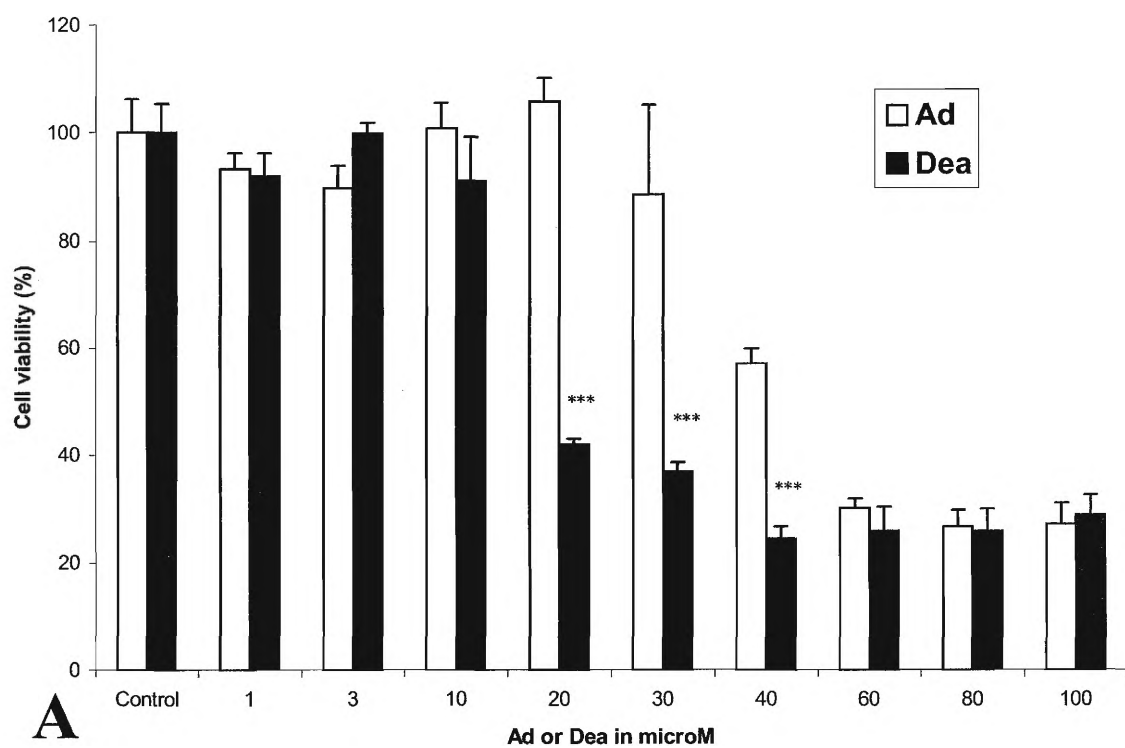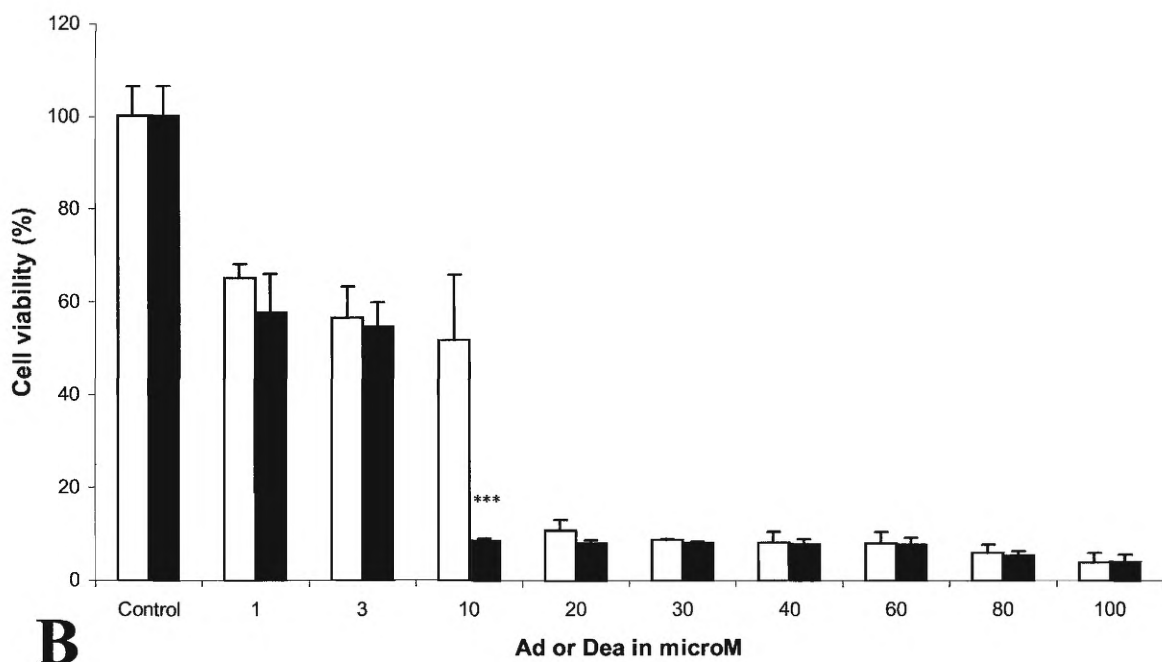

Fig. 12. The effect of amiodarone on apoptosis in SP-2 cells. Amiodarone-induced DNA fragmentation analysis (B) was performed by separating the total DNA content of SP-2 cells exposed to different concentrations of Ad for 24 hours by agarose gel electrophoresis. Lane 1: Marker; lane 2: no Ad; lane 3: 1 μM Ad; lane 4: 3 μM Ad; lane 5: 10 μM Ad; lane 6: 30 μM Ad;
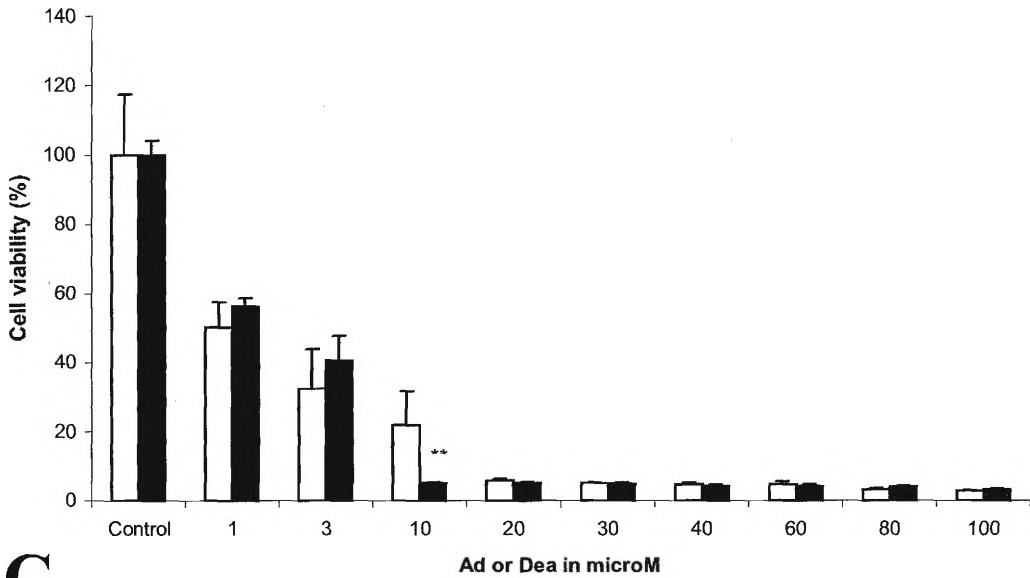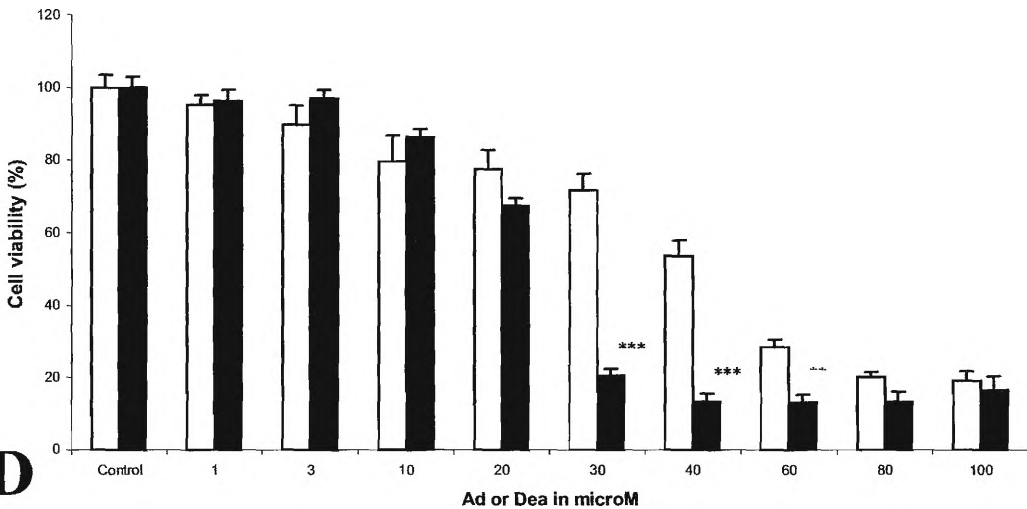
34

H9C2

BRL-3A

WRL-68

C

PANC-1

D

Fig. 13. The effect of amiodarone and desethylamiodarone on viability of cell lines. The effect of amiodarone (open bars) and desethylamiodarone (filled bars) on viability of H9C2 (A), BRL-3A (B), WRL-68 (C) and HeLa cells (D) were detected by the formation of water insoluble blue formasan dye from the yellow mitochondrial dye, MTT$^+$ by the functionally active mitochondria of the cells. The cells were exposed to different concentrations of amiodarone or desethylamiodarone for 48 hours before the addition of the MTT$^+$ dye. Data represents average ± S.E.M. of three independent experiments running in 4 parallels. **, significant difference (p < 0.01; mean ± S.E.M., paired t test); ***, significant difference (p < 0.001; mean ± S.E.M., paired t test) of amiodarone from equimolar concentrations of desethylamiodarone.

36

When H9C2 cardiomyocytes were exposed to different concentrations of amiodarone, desethylamiodarone or FCCP for only 1h (Fig. 14.), the results detected by the formation of
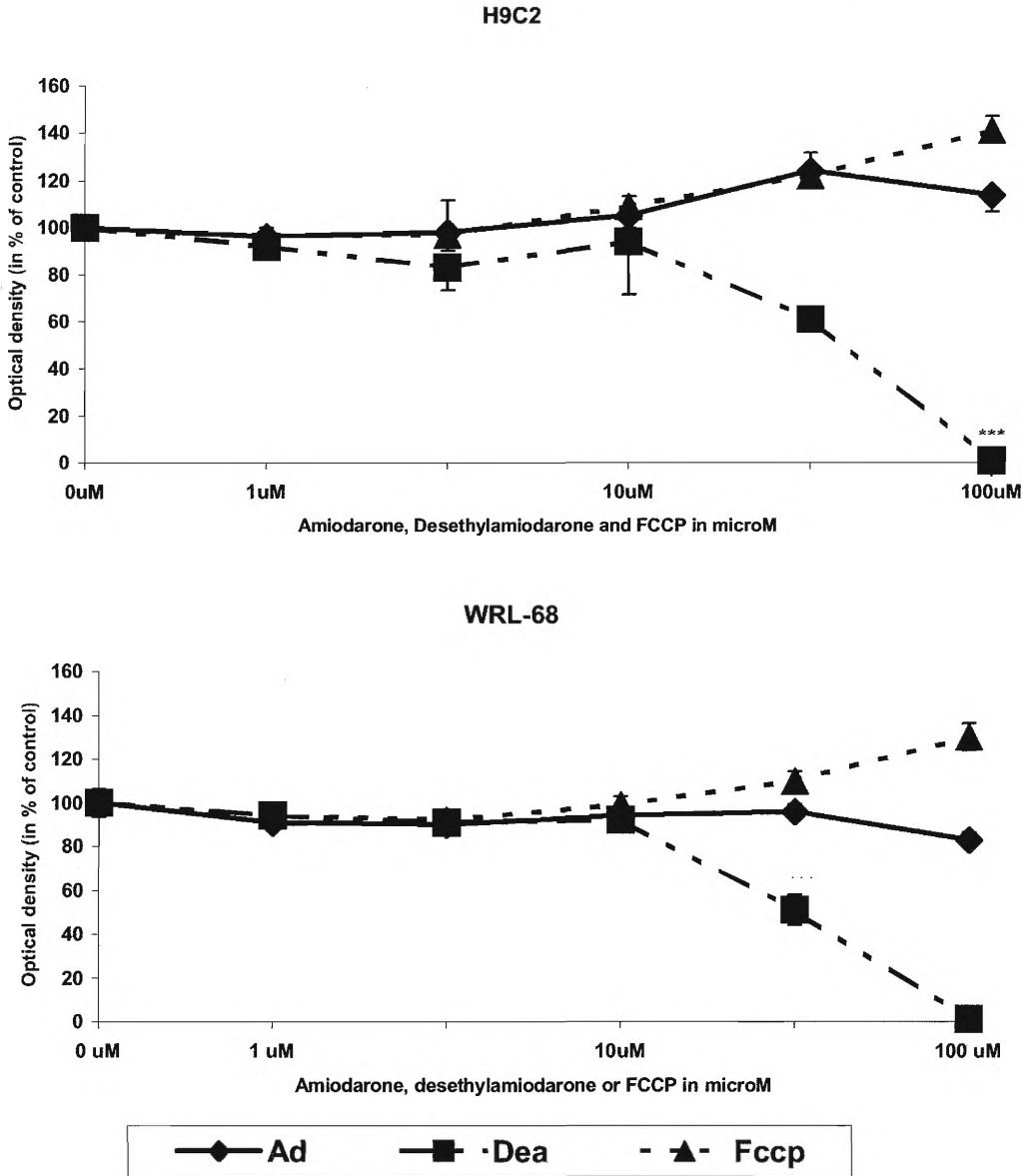
H9C2

WRL-68

Fig. 14. The effect of amiodarone, desethylamiodarone and FCCP on the cellular respiration. The effect of amiodarone, desethylamiodarone and FCCP on respiration of H9C2 (A) and WRL-68 (B) cells were detected by the formation of water insoluble blue formasan dye from the yellow mitochondrial dye, MTT^+ by the functionally active mitochondria of the cells. The cells were exposed to different concentrations of amiodarone, desethylamiodarone or FCCP for 1 hours before the addition of the MTT^+ dye. Data represents average ± S.E.M. of three independent experiments running in 4 parallels. +++, significant difference ($p < 0.001$; mean ± S.E.M., paired t test) of FCCP from equimolar concentrations of amiodarone; ***, significant difference ($p < 0.001$; mean ± S.E.M., paired t test) of desethylamiodarone from equimolar concentrations of amiodarone.

water insoluble blue formasan dye from the yellow mitochondrial dye, MTT^+ by the functionally active mitochondria reflect the respiratory state, rather than the number of viable cells. Amiodarone, up to the concentration of 30 μM, exerted an uncoupling effect as indicated by the increase of optical densities, similarly to that of the equimolar concentrations of FCCP, a widely used uncoupling agent. However, at the concentration of 100 μM, the stimulatory effect of amiodarone declined significantly ($p < 0.001$), when compared to equimolar concentrations of FCCP (114% ± 7 vs 141% ± 6). Desethylamiodarone did not exhibit any stimulatory effect on the respiration, when present in low concentrations, whereas it significantly ($p < 0.001$) decreased the MTT^+ formation, when compared to equimolar amount of amiodarone above the concentration of 10 μM. In WRL-68 liver cells, amiodarone, did not show any stimulatory effect up to the concentration of 30 μM, while it decreased the respiration, when present in higher concentration. The effect of both desethylamiodarone and FCCP on the respiration of WRL-68 were similar like in the case of H9C2, with desethylamiodarone showing inhibition, while FCCP manifesting an uncoupling effect above the concentration of 10 μM. The values of the optical densities in this concentration range for both desethylamiodarone and FCCP were significantly different ($P < 0.001$) from those of the equimolar concentrations of amiodarone.

Effect of amiodarone and desethylamiodarone on the energy metabolism during ischemia-reperfusion in perfused hearts. Concentrations of high-energy phosphate intermediates were monitored during ischemia-reperfusion in Langendorff-perfused hearts by using ^{31}P NMR spectroscopy (Fig. 15.). In order to study the effect of amiodarone or desethylamiodarone on the energy-metabolism of the perfused hearts, a single i.v. injection of 20 mg/kg amiodarone or 20 mg/kg desethylamiodarone was administered to a group of rats 30 min before the start of the heart-perfusion, a protocol that was previously reported to be optimal for cardioprotection by amiodarone. Thirty minutes of global ischemia induced the disappearance

38

of creatine phosphate and ATP, and a gradual increase of inorganic phosphate signal. During reperfusion, all hearts restarted working, while creatine phosphate concentrations in hearts of sham-operated animals recovered to 35% ± 4 of their normoxic
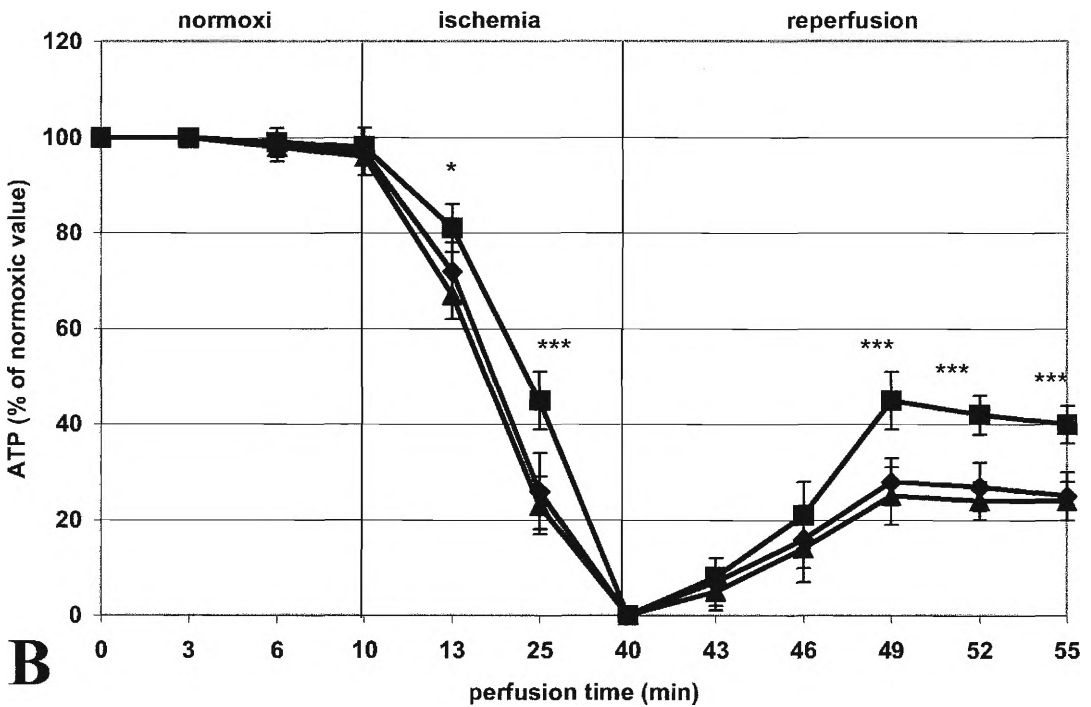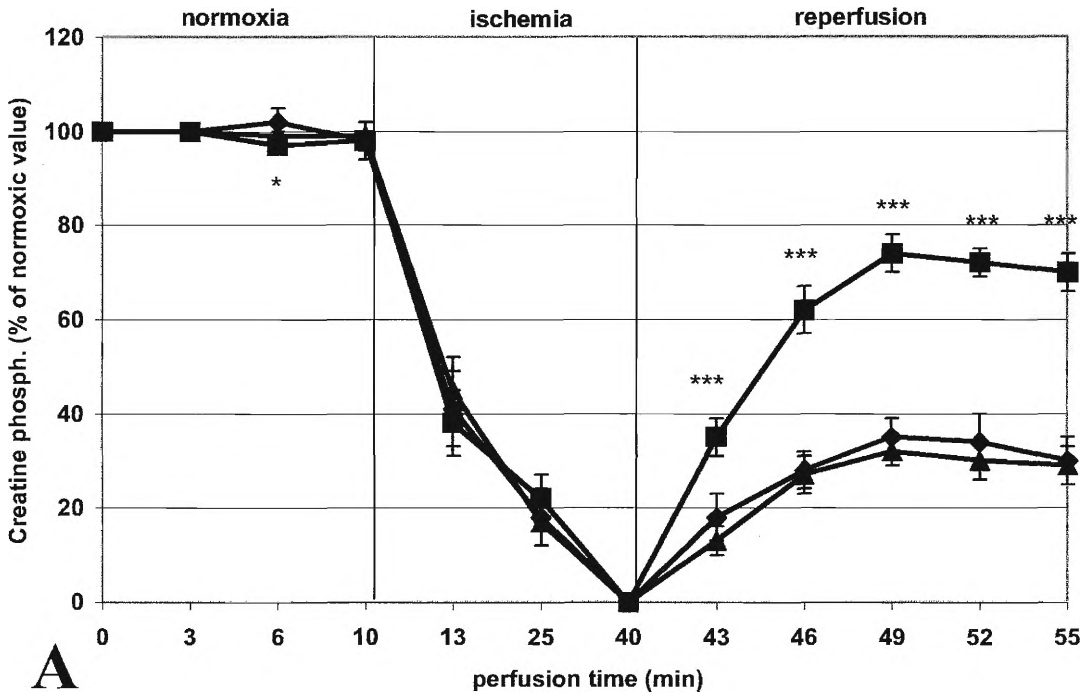
level. Amiodarone pretreatment resulted in a significantly higher recovery ($p < 0.001$) of creatine phosphate concentrations during the ischemia-reperfusion cycle (74% ± 6) when compared to control (35% ± 4), while the pretreatment with desethylamiodarone had no significant effect on the recovery of creatine phosphate concentration following ischemia (32% ± 4). In addition, amiodarone pretreatment slightly but significantly ($p < 0.05$) delayed the decrease of ATP concentrations during ischemia, while significantly ($p < 0.001$) improved
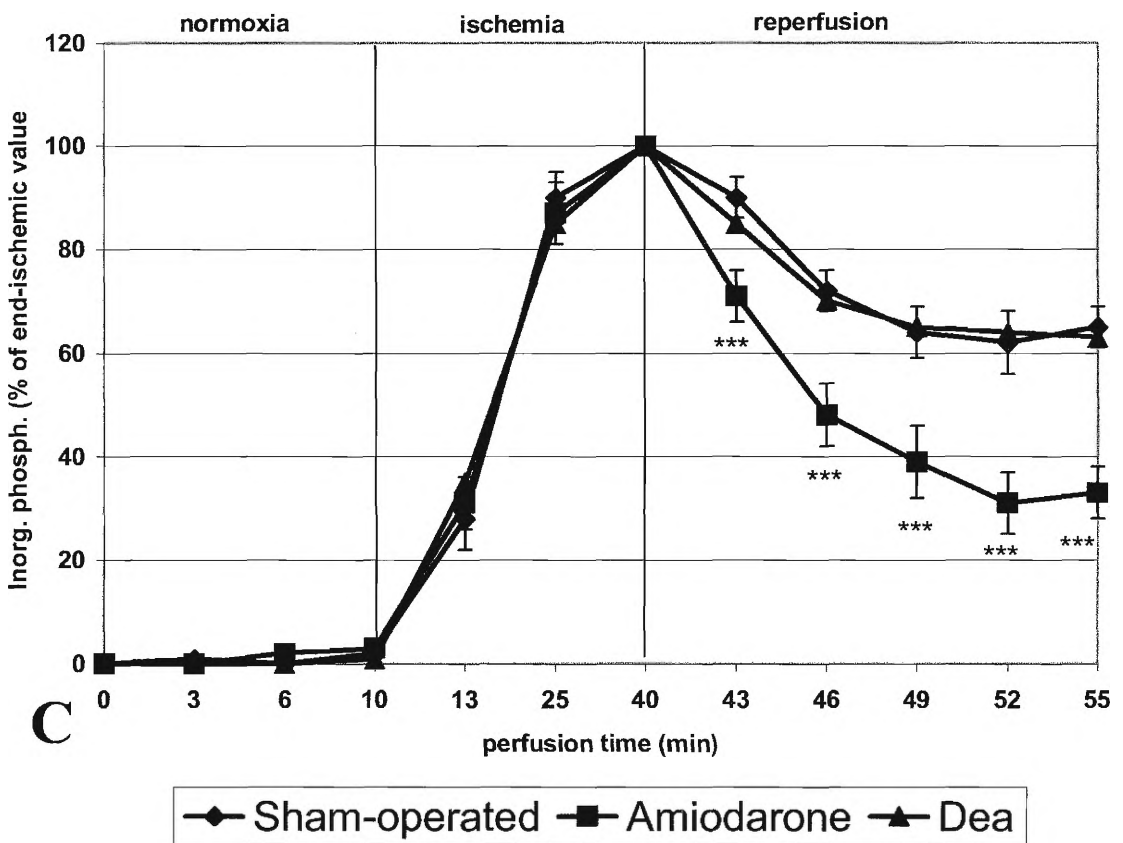
Fig. 15. The effect of amiodarone on the high-energy phosphate metabolism in Lagendorff-perfused rat hearts. Groups of 5 rats were treated by a single shot of physiological salt solution (sham-operated) or amiodarone 20 mg/kg iv. 30 min before sacrifice. Their hearts were removed, applied to a Langendorff perfusion apparatus which was inserted into the magnet of an NMR spectrometer. Concentrations of creatine phosphate (A), ATP (B) and inorganic phosphate (C) were measured *in situ* by ^{31}P NMR spectroscopy in the perfused hearts subjected to 30 min of ischemia followed by 15 min of reperfusion. Data represents average ± S.E.M. Note that the time axis is not proportional.

the recovery of ATP level (45% ± 6 vs. 28% ± 5). The pretreatment with desethylamiodarone had no significant effect on the recovery of ATP level (28% ± 5) when compared to control. Amiodarone pretreatment facilitated the significantly (p < 0.001) faster and more complete utilization of inorganic phosphate (31% ± 6 vs. 62% ± 6) during reperfusion. The pretreatment with desethylamiodarone did not prove to be effective in the utilization of inorganic phosphate (63% ± 4).

Discussion.

We observed that Taxol induced large amplitude swelling of mitochondria, the dissipation of mitochondrial membrane potential, opening of the permeability transition pore as detected by enzymatic method and on cytochrome-c release, all of which are regarded characteristic features of MPT. Our results indicate that Taxol, in a concentration dependent manner induced a CsA-sensitive permeability transition in isolated rat liver mitochondria. Permeability transition inducing effect of paclitaxel was not tissue specific, since paclitaxel induced swelling and dissipation of $\Delta\Psi$ was demonstrated in mitochondria isolated from not only rat liver, but heart, kidney, brain as well as from BRL-3A and HepG-2 cell lines. We used isolated mitochondria purified by Percoll-gradient centrifuging to exclude any indirect mechanism that could be involved in the effect of paclitaxel on MPT. These indicate, that paclitaxel – apart from previously described mechanisms (Torres and Horowitz, 1998) – also affects the mitochondria through direct interaction. The MPT inducing effect of paclitaxel was also verified in cell lines using fluorescent dyes.

Paclitaxel induced ROS formation in isolated mitochondria in a concentration dependent manner that could not be inhibited by CsA. Furthermore, the substances that attenuated ROS formation did not affect paclitaxel-induced MPT. These results suggest that MPT-inducing and ROS formation-inducing effect of paclitaxel in isolated mitochondria are mediated by separate mechanisms. Paclitaxel induced ROS formation was about significantly more intense in the lipid than in the aquous phase, suggesting that the ROS production was localized mainly in the mitochondrial membrane. Paclitaxel induced ROS formation with a similar rate either in the presence or absence of respiratory complex inhibitors, except for KCN, since in the presence of KCN paclitaxel failed to initiate mitochondrial ROS

production. These suggests that pactitaxel interfered with the rexod reactions of cytochrome-oxidase resulting in a cytochrome-oxidase activity dependent ROS production.

Both amiodarone and desethylamiodarone have damaging effect on extracardiac tissues (Amico et al., 1984; Martin and Howard, 1985; Card et al., 1998). While the reports on the effect of amiodarone on cardiac functions following ischemia-reperfusion have been variable (Nokin et al., 1987; Moreau et al., 1999), there is hardly any data about the effect of desethylamiodarone amid these circumstances. Therefore we monitored real time *in situ* concentrations of ATP, creatine phosphate and inorganic phosphate during ischemia-reperfusion of Langendorff-perfused rat hearts by ^{31}P-NMR spectroscopy. Our results show that amiodarone pretreatment resulted in a faster and more complete recovery of the high-energy phosphate concentrations and had a significant protecting effect on the energy metabolism of perfused hearts during ischemia-reperfusion. It's effect in preventing the ischemia-reperfusion induced release and nuclear translocation of AIF was also observed. However desethylamiodarone pretreatment had no protective effect neither on high energy phosphates nor on the AIF translocation. Extracardiac cell lines had an enhanced sensitivity toward amiodarone toxicity: amiodarone did not present sign of apoptosis in H9C2 cells whereas it showed DNA fragmentation in the extracardiac cell line SP-2 in the same concentration range. Furthermore, desethylamiodarone also was more toxic than amiodarone when tested in all cell lines. The observation, that amiodarone protected the energy metabolism in perfused hearts suggested, that the cardioprotectivity of the drug could be consequence of it's direct mitochondrial effect, by influencing the $\Delta\Psi$, the ROS production, the respiration or the MPT. Therefore we studied the direct effect of the drugs on isolated, mitochondria from rat liver and heart. Unlike paclitaxel, that induced MPT, we revealed that amiodarone has a mixed effect of mitochondrial functions. In low concentrations it stimulated state 4 respiration due to an uncoupling effect, inhibited the Ca^{2+}-induced mitochondrial

swelling, while it dissipated the $\Delta\Psi$. However at higher concentrations it exerted and inhibitory effect on the mitochondrial respiration, and simultaneously induced a mitochondrial swelling, that was not inhibited by CsA. In contrast to this, desethylamiodarone did not stimulate state 4 respiration, did not inhibit the Ca^{2+}-induced mitochondrial permeability transition and did not induce the collapse of $\Delta\Psi$ in low concentrations, while at higher concentrations, similar to amiodarone, it induced a mitochondrial swelling that was not inhibited by CsA and inhibited the respiration. We also found, that FCCP, a widely used uncoupling agent, inhibits the Ca^{2+}-induced mitochondrial swelling, while it dissipated the $\Delta\Psi$. Amiodarone similarly to FCCP exhibits uncoupling effect, inhibits swelling and dissipates the $\Delta\Psi$. A theory suggests, that during uncoupling, the mitochondrial respiratory chain works more efficiently, leading to less leakage of electrons and thus to lower levels of ROS generation (Budd et al., 1997), obscuring the mechanism by which FCCP or lower membrane potential promotes pore opening. Previous reports (Ribeiro et al., 1997; Di Matola et al., 2000), and our findings that amiodarone does not induce ROS production in isolated mitochondria is also in accord with this theory.

The beneficial properties of amiodarone are due to the presence of its ethyl group, since it's major metabolite, desethylamiodarone, does not exhibit the cardioprotective and beneficial mitochondrial features of the parent drug. In higher concentrations, amiodarone as well as desethylamiodarone, besides inhibiting the mitochondrial respiration can induce a CsA independent mitochondrial swelling, thus contributing to the toxic property of the drug. While both amiodarone and desethylamiodarone have similar antiarrhythmic properties, only amiodarone possesses with cardioprotective effect, and the frequently manifesting side effects during long-term amiodarone therapy could be related, at least in part, to the accumulation of desethylamiodarone.

List of Publications

Publications supporting the dissertation:

Varbiro G., Toth A., Tapodi A., Veres B., Gallyas F., Sumegi B.: Protective effect of amiodarone but not N-desethylamiodarone on postichemic hearts by the inhibition of mitochondrial permeability transition. **J. Pharm. Exp. Ther**. (2003) submitted.

Varbiro G., Toth A., Tapodi A., Veres B., Gallyas F., Sumegi B.: The concentration dependent mitochondrial effect of amiodarone. **Biochem. Pharmacol.** (2003) 65(7):1115-28.

Varbiro G., Veres B., Gallyas F., Sumegi B.: Direct effect of taxol on free radical formation and mitochondrial permeability transition. **Free Rad. Biol. Med.** (2001) 31(4):548-58

Other publications:

Veres B., Gallyas F., *Varbiro G.*, Berente Z., Osz E., Szekeres G., Szabo C., Sumegi B.: Decrease of the inflammatory response and induction of the Akt/protein kinase B pathway by poly-(ADP-ribose) polymerase 1 inhibitor in endotoxin-induced septic shock. **Biochem. Pharmacol.** (2003) 65(8):1373-82.

Sümegi B., Rablóczky G., Rácz I., Tory K., Bernáth S., *Varbiro G.*, Gallyas F. & Literáti Nagy P.: Protective effect of PARP inhibitors against cell damage induced by antiviral and anticancer drugs. (In.: **Cell Death: The Role of PARS**, Szabó Cs. Eds. CRC Press, 2000)

Csere, P., *Varbiro, G.*, Sumegi, B., Mozsik, G.: AIDS treatment and the shock protein level in the gastrointestinal tract. **Inflammopharm** (1997) 5:83-91

Csere, P., *Varbiro, G.*, Sumegi, B., Mozsik, G.: AIDS treatment and the shock protein level in the GI tract. In: Gagniella T., Mozsik G., Rainsford K. D. (Eds).
Biochemical Pharmacology as Approach to Gastrointestinal Disease: From Basic Science to Clinical Perspectives. Kluwer Academic Publisher, pp.287-295 (1997)

Abstracts, posters and presentations supporting the dissertation:

Varbiro, G., Veres, B., Gallyas, F., Sumegi, B.: The effect of taxol on liver mitochondrial free radical formation and mitochondrial permeability transition. (Abstract) **Z. Gastroenterologie** 5:428 (2001)

Varbiro, G., Veres, B., Gallyas, F., Sumegi, B., The effect of taxol on liver mitochondrial free radical formation and mitochondrial permeability transition. Balatonaliga, 43rd Annual Meeting of the Hungarian Society of Gastroenterology, 2001. June 5-9.

Varbiro, G., Veres, B., Gallyas, F., Tapodi, A., Sumegi, B.: A taxol közvetlen hatása a mitokondriális permeability transitionra és a szabadgyökképződésre. Sümeg, XXXI. Membrán-Transzport Konferencia, 2001. Május 22-25.

Tapodi, A., Veres, B., *Varbiro, G.*, Gallyas, F., Sumegi, B.: Az amiodarone mitokondriális hatásai. Sümeg, XXXI. Membrán-Transzport Konferencia, 2001. Május 22-25.

Jakus P., Tapodi A., *Varbiro G.*: Amiodarone indukálta génexpressziós változások analízise DNS-chip technikával. Pécs, A Pécsi Akadémiai Bizottság Sejtbiológiai Munkabizottságának Doktorandusz Szimpóziuma, 2002. december 11.

Tapodi A., Veres B., *Varbiro G.*, ifj. Gallyas F., Sumegi B.: Az amiodaron bifázisos mitokondriális hatásai. Siófok, X. Sejt- és Fejlődésbiológiai Napok, 2002. Március 27-29.

Veres B., *Varbiro G.*, Gallyas F., Sumegi B.: A taxol direkt hatása a mitokondriális szabadgyök képződésre és a permeability transitionra. Pécs, A Magyar Szabadgyök Kutató Társaság I. Kongresszusa, 2001. Április 5-7

Gallyas F., *Varbiro G.*, Veres B., Tapodi A., Sumegi B.: A Taxol közvetlen módon gyakorol hatást egyes mitokondriális funkciókra. Debrecen, IX. Sejt- és Fejlődésbiológiai Napok, 2001. Január 21-24

Varbiro G., Veres B., Gallyas F., Sumegi B.: Amiodarone, egy III tipusu anti-arrhytmias vegyulet hatasása a mitochondriális funkciokra. Pecs, VIII. Sejt- és Feljődés Biológiai Napok, 2000. Január 17-19

Other abstracts, posters and presentations

Varbiro G., Tapodi A., Veres B., Gallyas F. Jr., Sumegi B.: The induction of COX-2 expression through an NFkB dependent pathway in liver cells by amiodarone. (Abstract) **Z. Gastroenterologie** 5: (2002)

Csere, P., *Varbiro, G.*, Sumegi, B., Mozsik, G.: Has the AIDS treatment effect on the whole GI tract in heat shock protein level? (Abstract) **Dig Dis Sci** 1996 Feb;41(2):442

Szabo, J., *Varbiro, G.*: The response of odontoblasts on the injury of epithelial integrity. (Abstract) **Dig Dis Sci** 1996 Feb;41(2):438

Varbiro, G., Debreceni, B., Csere, P., Sumegi, B., Mozsik, G.: The role of heat shock proteins in the gastric cytoprotection (Abstract) **Z. Gastroenterologie** 5:388 (1996)

Csere, P., Debreceni, B., *Varbiro, G.*, Mozsik, G., Sumegi, B.,Kispal, G.:Function of the mitochondrial multi-drug resistance transporter homolog, Atm1p (Abstract) **Z. Gastroenterologie** 5:306 (1996)

Varbiro, G., Debreceni, B., Csere, P., Sumegi, B., Mozsik, G.: Analysis of Heat shock proteins with monoclonal antibodies in rat lingual and buccal mucosa following2`,3` dideoxycytidine (ddC) treatment (Abstract) **Z. Gastroenterologie** 5:314 (1995)

Veres B., Gallyas F. Jr., *Varbiro G.*, Berente Z., Osz E., Szekeres Gy., Szabo C., Sumegi B.: Pharmacological inhibition of poly(ADP-ribose) polymerase (PARP) protects mice against LPS-induced septic shock by the decreasing the inflammatory response and by enhancing the cytoprotective Akt/protein kinase B pathway. San Diego, CA., Experimental Biology 2003. Translating the Genome, 2003. April 11-15.

Varbiro, G., Tapodi, A., Veres, B., Gallyas, F., Sumegi, B.: The induction of COX-2 expression through an NFkB dependent pathway in liver cells by amiodarone Balatonaliga, 44rd Annual Meeting of the Hungarian Society of Gastroenterology, 2002. June 4-8.

Veres B., Tapodi A., *Varbiro G.*, ifj. Gallyas F., Sumegi B.: PARP-gátlók hatása az LPS indukálta szepszisre. Sümeg, XXXII. Membrán-Transzport Konferencia, 2002. Május 21-24.

Tapodi A., Veres B., *Varbiro G.*, ifj. Gallyas F., Sumegi B.: PARP-gátlók hatása oxidatív stresszben. Sümeg, XXXII. Membrán-Transzport Konferencia, 2002. Május 21-24.

Veres B., *Varbiro G.*, Tapodi A., ifj. Gallyas F., Sumegi B.: PARP-gátlók hatása a szeptikus sokkra. Siófok, X. Sejt- és Fejlődésbiológiai Napok, 2002. Március 27-29.

Varbiro, G., Debreceni, B., Csere, P., Sumegi, B., Mozsik, G.: The role of heat shock proteins in the gastric cytoprotection. Balatonaliga, 39th Annual Meeting of the Hungarian Society of Gastroenterology, 1996

Csere, P., Debreceni, B., *Varbiro, G.*, Mozsik, G., Sumegi, B.,Kispal, G.:Function of the mitochondrial multi-drug resistance transporter homolog, Atm1p. Balatonaliga, 39th Annual Meeting of the Hungarian Society of Gastroenterology, 1996

Varbiro, G., Debreceni, B., Csere, P., Sumegi, B., Mozsik, G.: Analysis of Heat shock proteins with monoclonal antibodies in rat lingual and buccal mucosa following2`,3` dideoxycytidine (ddC) treatment. Balatonaliga, 38th Annual Meeting of the Hungarian Society of Gastroenterology, 1995

Ifj. Gallyas F., Jun-Ichi Satoh, Tapodi A., *Varbiro G.*, Veres B.: Neurotranszmitter szintézis immortalizált sejtvonalakban. Siófok, X. Sejt- és Fejlődésbiológiai Napok, 2002. Március 27-29.

Gallyas F., *Varbiro G.*, Sumegi B.: Transzfekcio gátlása Poli-(ADP-ribóz) polimeráz inhibitorokkal emlős sejtvonalban. Pécs, VIII. Sejt- és Feljődés Biológiai Napok, 2000. Január 17-19

Gallyas F., *Varbiro G.*, Sumegi B.: Retrovirus-mediálta gén-inzerció gátlása Poli-(ADP-ribóz) polimeráz inhibitorokkal emlős sejtvonalban. Pécs, A Magyar Humángenetikai Társaság II. Kongresszusa, 1999 augusztus 25-28

Csere, P., *Varbiro, G.*, Sumegi, B., Mozsik, G.: Has the AIDS treatment effect on the whole GI tract in heat shock protein level? Pécs, IUPHAR symposium, 1995

Szabo, J., *Varbiro, G.*:The response of odontoblasts on the injury of epithelial integrity. Pécs, IUPHAR symposium, 1995

References.

Almeida A and Medina JM. A rapid method for the isolation of metabolically active mitochondria from rat neurons and astrocytes in primary culture. *Brain Res Brain Res Protoc* 1998;2:209-14.

Amico JA, Richardon V, Alpert B and Klein I. Clinical and chemical assessment of thyroid function during therapy with amiodarone. *Arch Intern Med* 1984;144:487-90.

Beltran B, Quintero M, Garcia-Zaragoza E, O'Connor E, Esplugues JV and Moncada S. Inhibition of mitochondrial respiration by endogenous nitric oxide: a critical step in Fas signaling. *PNAS* 2002;99:8892-97.

Bernardi P. Mitochondrial Transport of Cations: Channels, Exchangers, and Permeability Transition. *Physiol Rev* 1999;79:1127-55.

Borutaite V and Brown GC. Mitochondria in apoptosis of ischemic heart. *FEBS Letters* 2003;541:1-5.

Budd SL, Castilho RF and Nicholls DG. Mitochondrial membrane potential and hydroethidine-monitored superoxide generation in cultured cerebellar granule cells. *FEB Lett* 1997;415:21-24.

Card JW, Lalonde BR, Rafeiro E, Tam AS, Racs WJ, Brien JF, Bray TM and Massey TE Amiodarone-induced disruption of hamster lung and liver mitochondrial function: lack of association with thiobarbituric acid-reactive substance production. *Toxicol Lett* 1998;98:41-50.

Cassarino DS, Parks JK, Parker Jr WD and Benett Jr JP. The parkinsonian neurotoxin MPP[+] opens the mitochondrial permeability transition pore and releases cytochrome c in isolated mitochondria via an oxidative mechanism. *Biochim Biophys Acta* 1999;1453:49-62.

Chen G and Goddel DV. TNF-R1 signalling: a beautiful pathway. *Science* 2002;296:1634-35.

Cory S and Adams JM. The Bcl2 family: regulators of the cellular life-or-death switch. *Nat Rev Cancer* 2002;2:647-56.

D'Aurelio M, Pallotti F, Barrientos A, Gajewski CD, Kwong JQ, Bruno C, Beal MF and Manfredi G. In vivo regulation of oxidative phosphorylation in cells harboring a stop-codon mutation in mitochondrial DNA-encoded cytochrome c oxidase subunit I. *J Biol Chem* 2001;276:46925-32.

Di Matola T, D`Acsoli F, Fenzi G, Rossi G, Martino E, Bogazzi F and Vitale M. Amiodarone induces cytochrome c release and apoptosis through a iodine-independent mechanism. *J Clin Endocrinol Metab* 2000;85:4323-30.

Elimadi A, Morin D, Albengres E, Chauvet-Monges AM, Allain V, Crevat A and Tillement JP. Differential effects of zidovudine and zidovudine triphosphate on mitochondrial permeability transition and oxidative phosphorilation. *Br J Pharmacol* 1997;121:1295-1300.

Ellenbogen KA, O'Callaghan WG, Colavita PG, Smith MS and German LD. Cardiac function in patients on chronic amiodarone therapy. *Am Heart J* 1985;110:376-81.

Evtodienko YV, Teplova VV, Sidash SS, Ichas F and Mazat JP. Microtubule-active drugs suppress the closure of the permeability transition pore in tumor mitochondria. *FEBS Letters* 1996;393:86-88.

Fiskum G. Mitochondrial participation in ischemic and traumatic neural cell death. *J Neurotrauma* 2000;17:843-55.

Garcia MV, Hernandez-Berciano R, Lopez-Mediavilla C, Orfao A and Medina JM. cAMP and Ca^{2+} involvement in the mitochondrial response of cultured fetal rat hepatocytes to adrenaline. *Exp Cell Res* 1997;237:403-9.

Gorczyca W, Gong J, Ardelt B, Traganos F and Darzynkiewicz Z. The cell cycle related differences in susceptibility of HL-60 cells to apoptosis induced by various antitumor agents. *Cancer Res* 1991;139:271-7.

Green DR and Reed JC, Mitochondria and Apoptosis. *Science* 1998;281:1309-12

Haldar S, Chintapalli J and Croce CM. Taxol induces *bcl-2* phosphorylation and death of prostate cancer cell. *Cancer Res* 1996;58:1253-5.

Haldar S, Jena N and Croce CM. Inactivation of *bcl-2* by Phosphorylation. *Proc Natl Acad Sci* 1995;92:4507-11.

Halmosi R, Berente Z, Osz E, Toth K, Literati-Nagy P and Sumegi B. Effect of poly-ADP-ribose-polymerase inhibitors on the ischemia-reperfusion induced oxidative cardiac injury and mitochondrial metabolism in Langendorff heart perfusion system. *Mol Pharmacol* 2000;59:1497-1505.

Horowitz SB. Mechanism of action of Taxol. *Trends Pharmacol Sci* 1992;13:34-36.

Ibrado AM, Liu L and Bhalla K. Bcl-xl overexpression inhibits progression of molecular events leading to paclitaxel-induced apoptosis of human acute myeloid leukemia HL-60 cells. *Cancer Res* 1997;57:1109-15.

Karlson JA, Hopkins RW, Moran JM and Karlson KE. Long-term amiodarone administration protects against global myocardial ischemia. *Ann Thorac Surg* 1990;50:575-8.

Korge P and Weiss JN. Thapsigargin directly induces the mitochondrial permeability transition. *Eur J Biochem* 1999;265:273-80.

Martin WJ and Howard DM Amiodarone-induced lung toxicity. In vitro evidence for the direct toxicity of the drug. *Am J Pathol* 1985;120:344-50.

Mattson MP. Apoptosis in neurodegenerative disorders. *Nat Rev Mol Cell Biol* 2000;1:120-9.

Moreau D, Clauw F, Martine L, Grynberg A, Rochette L and Demaison L. Effects of amiodarone on cardiac function and mitochondrial oxidative phosphorylation during ischemia and reperfusion. *Mol Cell Biochem* 1999;194:291-300.

Nokin P, Jungbluth L and Mouton J. Protective effects of amiodarone pretreatment on mitochondrial function and high energy phosphates in ischemic rat heart. *J Moll Cell Cardiol* 1987;19:603-14.

Penninger JM and Kroemer G. Mitochondria, AIF and caspase: rivaling for cell death execution. *Nat Cell Biol* 2003;5:97-99.

Remme WJ and van Hoogenhuyze DC. Hemodynamic profile of amiodarone during acute and long-term administration in patients with ventricular dysfunction. *Cardioscience* 1990;1:169-76.

Ribeiro SM, Campello AP, Nascimento AJ and Kluppel ML. Effect of amiodarone (AMD) on the antioxidant enzymes, lipid peroxidation and mitochondrial metabolism. *Cell Biochem Funct* 1997;15:145-52.

Schiff PB, Fant J and Horowitz SB. Promotion of microtubule assembly *in vitro* by Taxol. *Nature* 1979;277:665-7.

Schmitt JP, Schunkert H, Birnbaum DE and Aebert H. Kinetics of heat shock protein 70 synthesis in the human heart after cold cardioplegic arrest. *European Journal of Cardio-Thoracic Surgery* 2002;22:415-20.

Schneider WC and Hageboom GH. Further studies on the distribution of cytochrome c in rat liver homogenates. *J Biol Chem* 1950;183:123-8.

Sims NR. Rapid isolation on metabolically active mitochondria from rat brain and subregions using Percoll density gradient centriguration. *J Neurochem* 1990;55:698-707.

Singh BN and Vaughan Williams EM. The effect of amiodarone, a new anti-anginal drug, on cardiac muscle. *Br J Pharmacol* 1970;39:657-67.

Szabados E, Fisher MG, Gallyas F, Kispal Gy and Sumegi B. Enhanced ADP-ribosylation and its diminition by lipoamide following ischemia-reperfusion in perfused rat heart. *Free Rad. Biol. Med.* 1999;27:1103-13.

Torres K and Horwitz SB. Mechanisms of Taxol-induced cell death are concentration dependent. *Cancer Res* 1998;58:3620-26.

Wang X. The expanding role of mitochondria in apoptosis. *Genes Dev* 2001;15:2922-33.

Wolf BB and Green DR. Suicidal tendencies: apoptotic cell death by caspase family proteinases. *J Biol Chem* 1999;274:20049-52.

Zamzami N, Susin SA, Marchetti P, Hirsch T, Gomez-Monterrey L, Castedo M and Kroemer G. Mitochondrial control of nuclear apoptosis. *J Exp Med* 1996;183:1533-44.

Acknowledgement.

I would like to thank prof. Dr. Gyula Mózsik and prof. Dr. Balazs Sümegi the support, and guidance I received.

I would like to thank dr. Ferenc Gallyas Jr., associate professor the cooperation, assistance and advices.

I would also like thank the technical help I recieved fom László Girán, Bertalan Horváth and Helena Halász.

And last but not least I would like to thank my family the support and encouragment for completing my work.